CHALMERS
UNIVERSITY OF TECHNOLOGY

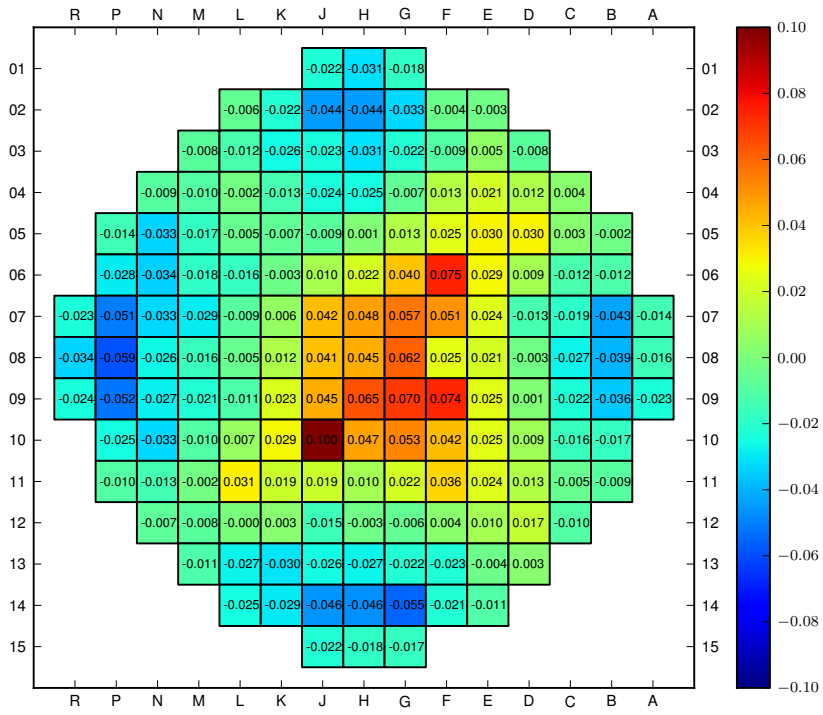


# Investigation of Deviations Between Measured and Calculated Peaking Factors at Ringhals 3

Master's Thesis in Nuclear Engineering

MARKUS MYBECK

Department of Applied Physics
CHALMERS UNIVERSITY OF TECHNOLOGY
Gothenburg, Sweden 2015

# Investigation of Deviations Between Measured and Calculated Peaking Factors at Ringhals 3

MARKUS MYBECK


CHALMERS
UNIVERSITY OF TECHNOLOGY

Department of Applied Physics
*Division of Nuclear Engineering*
Chalmers University of Technology
Gothenburg, Sweden 2015

Investigation of Deviations Between Measured and Calculated Peaking Factors at Ringhals 3
MARKUS MYBECK



Supervisor: Henrik Nylén, Ringhals AB
Examiner: Anders Nordlund, Division of Nuclear Engineering

CTH-NT-311
ISSN 1653-4662
Department of Applied Physics
Division of Nuclear Engineering
Chalmers University of Technology
SE-412 96 Gothenburg
Telephone +46-(31) 772 3083

Cover: Difference between measured and calculated $F_{\Delta H}$ values.

Typeset in LaTeX
Gothenburg, Sweden 2015

Investigation of Deviations Between Measured and Calculated Peaking Factors at Ringhals 3

MARKUS MYBECK
Department of Applied Physics
Chalmers University of Technology

# Abstract

The startup of cycle 32 for Ringhals 3 did not go as planned. A measurement at 97% power established that the limit for the radial peaking factor $F_{\Delta H}$, which is a measure of the radial power distribution in the core, had been exceeded by a small amount.

The simulations performed beforehand had predicted that all safety related parameters would stay within their limits during startup towards full power, which meant there were discrepancies between predictions and the real measurements. The purpose of this report is to understand the reasons for the deviations between measured and calculated values, and try to minimise them. The tools used are modern codes for cross-section generation (CASMO 4/5) along with a core simulator (SIMULATE 3/5) provided by Studsvik Scandpower.

The conclusion is that the error can be split into two parts. A large part is an asymmetric tilt that is likely caused by fuel bowing. The second part is a symmetric deviation that can be reduced by changing the neutron library and accounting for errors in the measurement of thermal power.

The recommendations are to load fresh fuel evenly distributed in the core to avoid large deviations in future cycles. Further study is also advised to better predict the effect of fuel bowing and to find more causes of the symmetric error.

Keywords: Ringhals 3, Peaking factor, Nuclear reactor, SIMULATE, CASMO, Symmetric, Asymmetric.

# Acknowledgements

I would sincerely like to thank my supervisors Henrik Nylén, Ulrik Svensson and Mattias Carlsson. Without them this thesis would not have been possible. The many questions answered and discussions about various topics have been vital to keeping the work going. The quality of the work has also been helped immeasurably with my supervisors really showing enthusiasm and helping to correct my mistakes.

Next I would like to thank Anders Nordlund who has acted my examiner during this work. Good ideas and support during the work has been a great help. I would also like to thank Rune Axelsson for giving me the opportunity to begin work on the thesis. Finally I would like to thank everyone at RTHH for making the work at Ringhals an enjoyable experience.

Markus Mybeck, Gothenburg, June 2015

# Contents

# List of Figures

# List of Tables

# List of abbreviations

**BA** . . . . . Burnable Absorber
**BOC** . . . . . Beginning Of Cycle
**BWR** . . . . . Boiling Water Reactor
**C##** . . . . . Reactor cycle number ##
**C4/5** . . . . . CASMO-4/5
**EOC** . . . . . End Of Cycle
**$F_{\Delta H}$** . . . . . Radial peaking factor
**GWd/MT** . . . . . Gigawatt-days per Metric Ton (of heavy metal)
**k-eff** . . . . . Effective neutron multiplication factor
**k-inf** . . . . . Infinite neutron multiplication factor
**PWR** . . . . . Pressurized Water Reactor
**RPF** . . . . . Relative Power Fraction
**S3/5** . . . . . SIMULATE-3/5

# 1
# Introduction

## 1.1 Ringhals Power Plant

The Ringhals nuclear power plant is the largest power plant in Scandinavia. It has 4 reactors, one boiling water reactor (BWR) and three pressurized water reactors (PWRs). The plant is located in south-west Sweden and generates about one fifth of the country's electrical energy production.

Ringhals 3 and 4 were built at the same time and have similar specifications. This work will focus on Ringhals 3. See Table 1.1 and Figure 1.1 for an overview of the reactor.

**Table 1.1:** Data for Ringhals 3 [1].

| Specification | Ringhals 3 |
|---|---|
| Manufacturer | Westinghouse |
| Start of commercial operation | September 1981 |
| Net power output | 1063 MW |
| Thermal power rating | 3135 MW |
| Operation pressure | 15.5 MPa |
| Steam temperature | 276 °C |
| Steam flow rate | 1670 kg/s |
| Number of fuel assemblies | 157 |
| Number of control rods | 48 |
| Fuel pin configuration | 17x17 |

The electricity in a PWR is generated in the secondary loop by turbines that are driven by superheated steam. Also present in the secondary loop is the steam generator and the condenser. Water is heated in the steam generator by water in the primary loop that is kept under high pressure. The primary loop also consists of the pressurizer and the reactor pressure vessel. The reactor pressure vessel contains the reactor core which is loaded with 157 fuel assemblies. These fuel assemblies are made up of a 17x17 grid of fuel pins and guide tubes for control rods and instrumentation.

The Ringhals PWRs are running on a cycle where about a third of the fuel is replaced about every twelve months. The cycles were numbered starting at cycle 1 and the cycle starting in 2014 for Ringhals 3 was cycle 32. The fresh fuel is much more reactive than the fuel removed and to be fuel efficient the entire core is reloaded in a

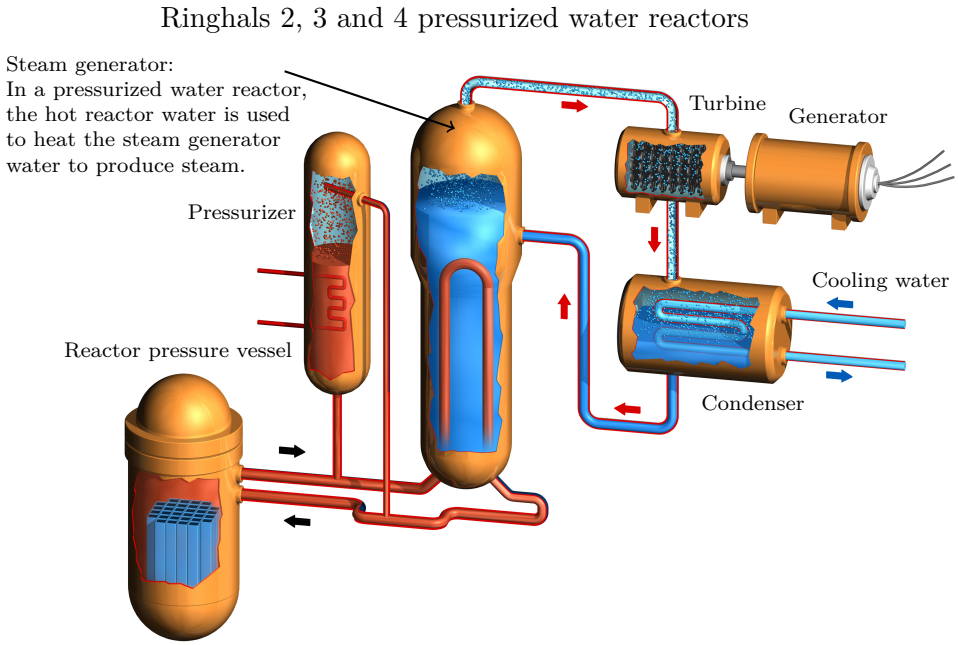


**Figure 1.1:** Overview of the Ringhals PWRs, created by Coloric, Varberg [1].

new pattern. Before new fuel is loaded simulations are performed to show that the new core layout will pass all safety criteria. During startup after the fuel change, control measurements are made at different power levels. These measurements are used to verify the simulations.

## 1.2 Background

The startup of cycle 32 for Ringhals 3 did not go as planned. A measurement at 97% power established that the limit for the hot channel enthalpy rise factor had been exceeded by a small amount. The hot channel enthalpy rise factor ($F_{\Delta H}$), in this work for simplicity referred to as the radial peaking factor, is a measure of the radial power distribution in the core. The consequences of this measurement was that the power had to be reduced and new measurements were performed to ensure that $F_{\Delta H}$ was below the limit. The reactor could not be run at full power until some time into the cycle due to this deviation which meant that production goals were impacted.

The simulations performed beforehand had predicted that all safety related parameters would stay within their limits during startup towards full power, which meant there were discrepancies between predictions and the real measurements. Figure 1.2 shows the difference between measured and calculated values for the radial power distribution (using a top-down view of the core). With a perfect model of the reactor every number in this plot would be 0.

It is clear that the real core developed a relatively higher power in the central part than predicted. In position J-10 the limit was exceeded, and it is also the position

with highest deviation. The $F_{\Delta H}$ differences seen in this plot have been investigated but no satisfactory explanation has been found.

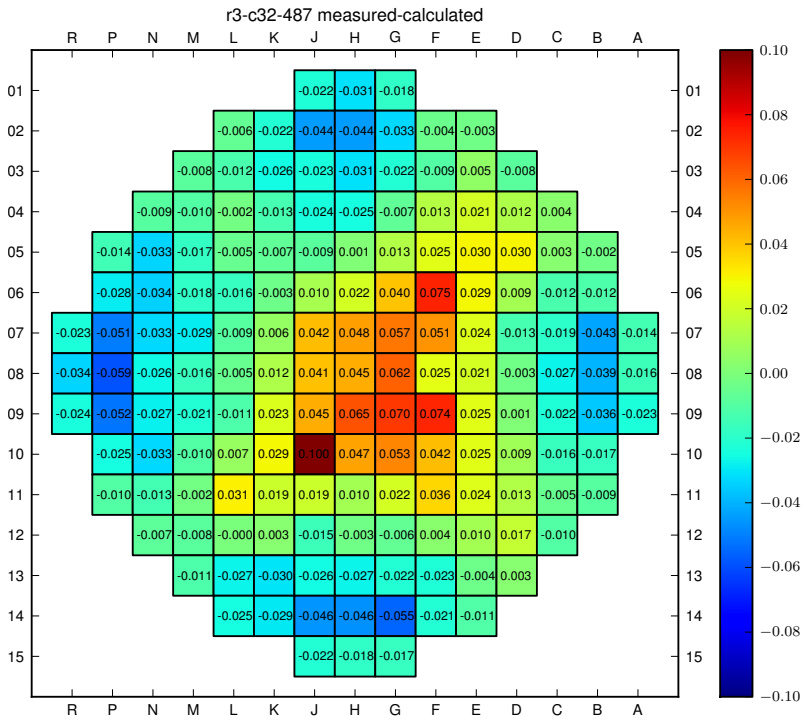


**Figure 1.2:** Absolute $F_{\Delta H}$ deviations, c32, *measured* − *calculated* values

## 1.3 Purpose and Project Aim

The purpose is to understand the reasons for the deviations between measured and calculated values, and try to minimise them. The tools used are modern codes for cross-section generation (CASMO 4/5) along with a core simulator (SIMULATE 3/5) provided by Studsvik Scandpower. The work was performed at Ringhals.

# 2
# Theory

This chapter will lay out the fundamentals of the theory behind the tools used in this thesis. It will also describe the software used and the equations used therein.

## 2.1 The Core Calculation Codes

The equation describing the physics of neutron transport is known and relatively straightforward. This equation is the Boltzmann (or transport) equation, see Equation 2.1 [2].

$$\left(\frac{1}{v}\frac{\partial}{\partial t} + \Omega \cdot \nabla + \Sigma(\mathbf{r}, E)\right) \Psi(\mathbf{r}, \mathbf{\Omega}, E, t) = (H\Psi)(\mathbf{r}, \mathbf{\Omega}, E, t) + (F\Psi)(\mathbf{r}, \mathbf{\Omega}, E, t) \quad (2.1)$$

The variables $v, \mathbf{r}, \mathbf{\Omega}, E, t$ are speed, position, solid angle, energy and time respectively. $\Psi(\mathbf{r}, \mathbf{\Omega}, E, t)$ is the angular neutron flux. On the left hand side is the rate of change, the in/out-flux of neutrons and the change by movement of the angular neutron flux $\Psi(\mathbf{r}, \mathbf{\Omega}, E, t)$. On the right hand side the production of neutrons from fission and the scattering from other groups are accounted for.

The drawback from this deterministic equation is the many variables that make it impractical to use in calculations. This is especially true for complex systems such as a nuclear reactor. The Boltzmann equation can be simplified into the two group time independent diffusion equation, see Equation 2.2.

$$\begin{aligned} \nabla D_1(\mathbf{r}) \nabla \mathbf{\Phi}_1(\mathbf{r}) + \left(\frac{v\Sigma_{f,1}(\mathbf{r})}{k_{eff}} - \Sigma_{a,1}(\mathbf{r}) - \Sigma_r(\mathbf{r})\right) \mathbf{\Phi}_1(\mathbf{r}) & \\ + \frac{v\Sigma_{f,2}(\mathbf{r})}{k_{eff}} \mathbf{\Phi}_2(\mathbf{r}) = 0 & \quad (2.2) \\ \nabla D_2(\mathbf{r}) \nabla \mathbf{\Phi}_2(\mathbf{r}) - \Sigma_{a,2}(\mathbf{r}) \Phi_2(\mathbf{r}) + \Sigma_r(\mathbf{r}) \Phi_1(\mathbf{r}) = 0 & \end{aligned}$$

Here $\Phi_g(\mathbf{r})$ is the scalar neutron flux and $D_g$ is the diffusion coefficient for the energy group g. $\Sigma_{(f,a,r),g}$ are the fission, absorption and removal macroscopic cross sections respectively. This equation is much less computationally expensive.

In this thesis CASMO-4 and CASMO-5, which solve the transport- and diffusion equations for cross section generation, have been used along with SIMULATE-3 and SIMULATE-5, which solve the diffusion equation with cross sections generated from CASMO. CASMO and SIMULATE are written in Fortran and use an input based around blocks of text called cards.

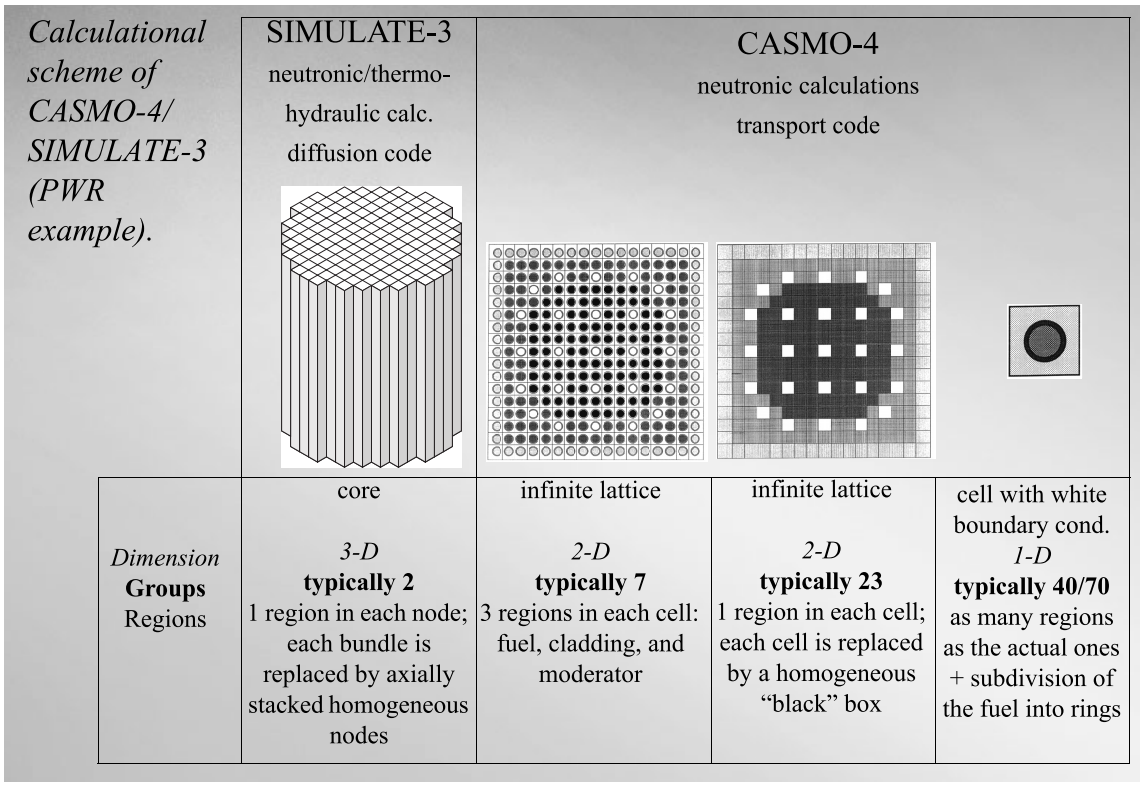


**Figure 2.1:** Calculation scheme of CASMO-4 and SIMULATE-3, from [3].

### 2.1.1 CASMO

CASMO is a transport theory code that performs burnup calculations on PWR and BWR assemblies. This is done in two dimensions with reflective boundaries and multiple neutron groups [4]. The calculation is performed in several steps where each steps increases the complexity of the geometry while reducing the number of energy groups, see Figure 2.1.

CASMO uses a neutron library for its calculations. There are several libraries used in the world that were developed using experimental data. The version of CASMO-4 used in this thesis is C4E 2.05.14_MROD which uses the JEF 2.2 library. CASMO-5 is version C5M 1.06 which uses the ENDF B VII library.

The data from CASMO is compiled into a library using CMSLINK. This library contains cross sections for the different fuel types at different burnup stages.

### 2.1.2 SIMULATE

SIMULATE uses the 2-group diffusion model to do time-independent calculations for the 3D core. This is done in nodes, for which SIMULATE treats the fuel assemblies as homogeneous with averaged material densities.

The entire core is set up in SIMULATE. New assemblies are assembled using different fuel types and the reflectors are defined. The assemblies are then placed in the correct loading pattern, and calculations are performed with input such as core power

and temperature/pressure. Neutronic and thermohydraulic iterations are performed in steady state. The progression of the cycle is accounted for by performing these calculations several times with the assembly cross sections being updated before every calculation. The burnup is calculated by recording the history of each assembly as the cycle progresses. Old assemblies already have their burnup history from previous cycles. [5].

The results from the calculations are in the form of averaged distributions, e.g. power, burnup, and specific safety related parameters. The SIMULATE versions used in this thesis were S3 6.09.14_VAT_12 and S5 1.08.001.

## 2.2 Peaking Factors

An important part of designing a loading pattern is to make sure the power distribution is as flat as possible in the core. This is because the maximum heat flux is a limiting factor and a flat power distribution will enable the reactor to run at full power with sufficient safety margins. To aid in designing the core several numbers are used to quantify the power distribution.

The total power peaking factor $F_Q$ is defined as the fraction between the highest power per rod length [W/cm] and the average power per rod length in the core. The radial peaking factor $F_{\Delta H}$ is the fraction between the hottest channels (between four fuel rods) enthalpy change and the average channel enthalpy change. This report will exclusively deal with the radial power distribution and thus $F_{\Delta H}$ will be the peaking factor of interest.

The peaking factors are not easy to measure. A nuclear reactor core is a harsh environment where sensitive detectors do not survive. Neutron flux is the only thing measured inside the core using movable detectors. This means that the measured power distribution is derived from measurements that are sensitive only to the local environment (a few rows of fuel rods). The neutron flux is related to the power level which means $F_{\Delta H}$ is approximated by the the maximum rod power divided by the overall rod power [6].

## 2.3 Use of Detectors

Ringhals 3 uses movable detectors to gather data inside the core. The core consists of 157 assemblies but not all of them are measured. The positions measured are located as seen in Figure 2.2. The detectors are inserted at the bottom of the core and moved through it to measure the neutron flux.

The peaking factors of the positions that are not measured have to be extrapolated from the measured points. This is performed in SIMULATE and it is worth keeping in mind that some patterns that are seen could possibly be explained by this.

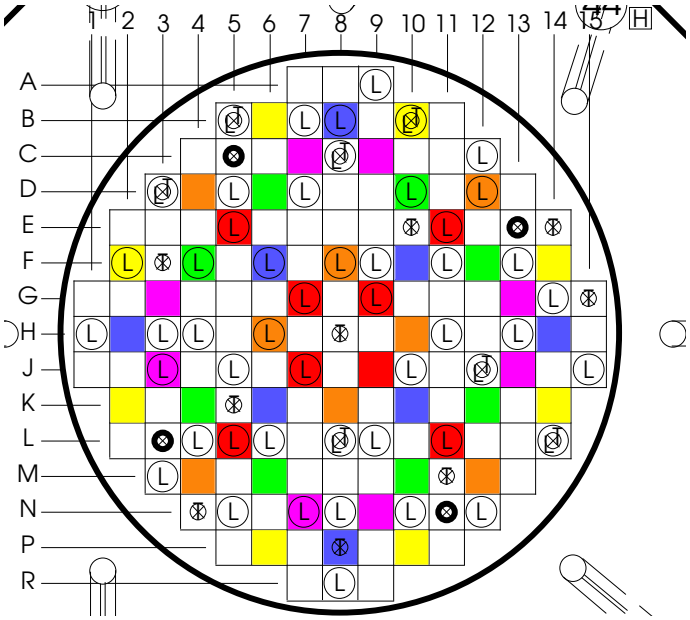


**Figure 2.2:** Schematic overview of the Ringhals 3 core. The (L) signifies the position has a measuring point for movable detectors. Note that the picture should be rotated 90 degrees to match the coordinate system used in this report.

### 2.3.1 Core Power Reconstruction

The detector used in the core does only measure the magnitude of the neutron flux. From the simulated power profile SIMULATE calculates the expected detector response. This value can now be compared to measurements.

In detector positions the ratio between the measured and calculated reaction rates are calculated as seen in Equation 2.3 [7].

$$R_{frac} = \frac{R_{detector}}{R_{Calculated}} \tag{2.3}$$

Where there is no detector, weighting factors have to be used to interpolate the power for the non-measured assembly. The weighting factor values are shown in Figure 2.3.

If a position is close to three detectors the measured power will be estimated from the calculated power and weighted with the three detectors weighting factors (w), see Equation 2.4. This adaptation procedure is performed with a function named ADAPT.

$$P_{meas} = P_{calc}\frac{R(1)_{frac}w(1)R(2)_{frac}w(2) + R(3)_{frac}w(3)}{w(1) + w(2) + w(3)} \tag{2.4}$$

| | | | | | |
|---|---|---|---|---|---|
| 1 | 0.667 | 0.333 | 0.0001 | 0.0001 | 0.0001 |
| 0.667 | 0.667 | 0.333 | 0.0001 | 0.0001 | 0.0001 |
| 0.333 | 0.333 | 0.333 | 0.0001 | 0.0001 | 0.0001 |
| 0.0001 | 0.0001 | 0.0001 | 0.0001 | 0.0001 | 0.0001 |
| 0.0001 | 0.0001 | 0.0001 | 0.0001 | 0.0001 | 0.0001 |
| 0.0001 | 0.0001 | 0.0001 | 0.0001 | 0.0001 | 0.0001 |

**Figure 2.3:** The default weighting factors. A detector is located in the 1 position.

# 3
# Methodology

This chapter describes the work that was done and the tools used to investigate the error that was caught in cycle 32. A big part of this is investigating whether the deviations found in cycle 32 was a random occurrence or something that could have been predicted.

## 3.1 Fluxmaps

One important tool when measuring the core is to perform fluxmaps, where the axial power distribution is measured for several radial positions in the core. Fluxmaps can be used for calibration against external detectors and core calculations. The data from the detectors is condensed into a 2D-plane to give a picture of the radial power distribution in the core. Since the parameter that exceeded its limit was $F_{\Delta H}$ that is the parameter that will be used the most. Coloured plots showing selected 2D-distributions in the core will be used a lot in this report for analysis.

The fluxmaps are taken at regular intervals during the cycle. The deviations tend to decrease during the cycle which means the biggest deviations will be present in the beginning of the cycle. Most of the fluxmaps shown in this report are the first fluxmap taken at full power for each cycle. The deviation values are presented with either absolute differences ($measured - calculated$ values) or relative differences ($(measured - calculated)/measured$ values).

## 3.2 Deviations in Historic Cycles

It is interesting to know if the kind of deviation seen in cycle 32 has also been present in previous cycles without causing a violation of the limit of some parameter. If that is the case a sound approach is to look for a common cause and if not differences can be examined.

Plotting cycles 25 to 32 with the radial fluxmap chart reveals some interesting information, see Figures 3.1 to 3.8. Cycle 31 and to some degree cycle 29 display the same kind of deviation as cycle 32, the core is hotter (higher relative power) than calculated in the middle. Cycle 30 does not have this clear deviation however. Another thing to note is that from cycle 27 onwards the edges of the main axis is noticeably cooler (lower relative power) than in cycle 25 and 26. These cooler edges can not be seen when plotting cycles earlier than 25 either, so from cycle 27 and onwards a phenomenon not previously observed for Ringhals PWRs is noticed.

Since the deviations are different for each cycles they are not an inherent property of the simulator. Instead the deviations seen in each cycle are either something that depends on the history of the assemblies or something that is independent from previous cycles and comes from cycle specific variables. A combination of the two is also possible.

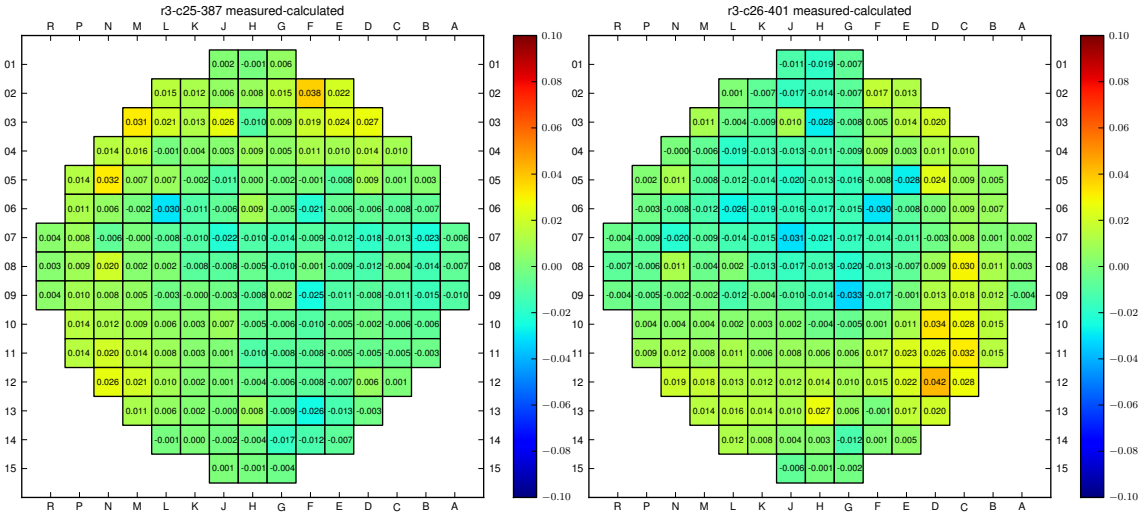


**Figure 3.1:** Absolute $F_{\Delta H}$ deviations, c25




**Figure 3.2:** Absolute $F_{\Delta H}$ deviations, c26

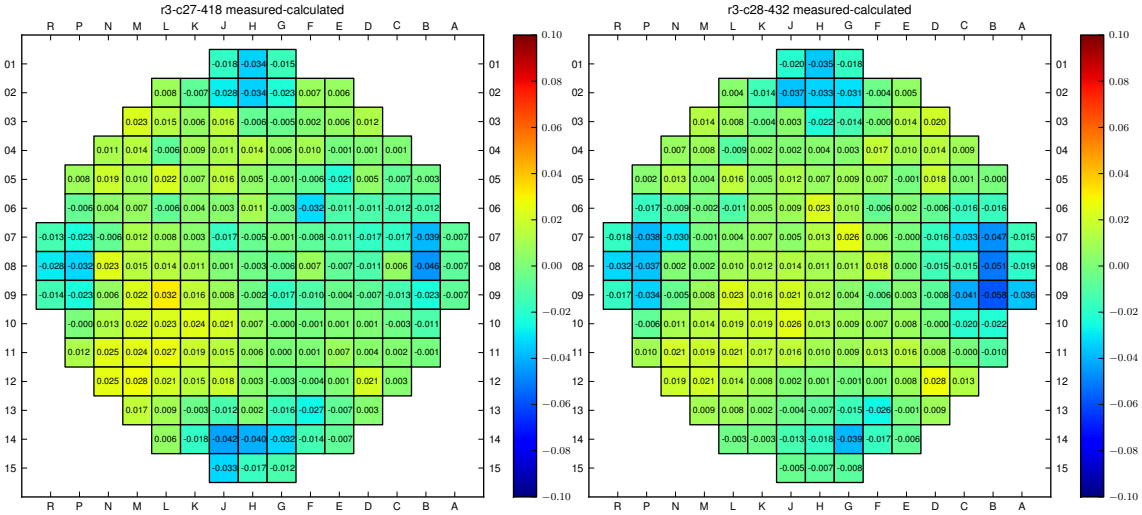


**Figure 3.3:** Absolute $F_{\Delta H}$ deviations, c27




**Figure 3.4:** Absolute $F_{\Delta H}$ deviations, c28

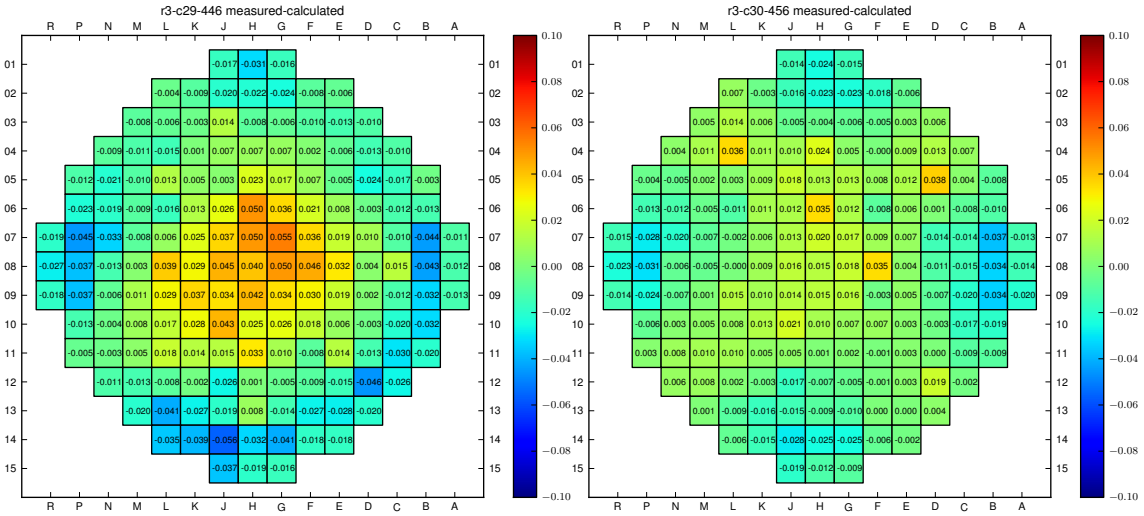


**Figure 3.5:** Absolute $F_{\Delta H}$ deviations, c29




**Figure 3.6:** Absolute $F_{\Delta H}$ deviations, c30

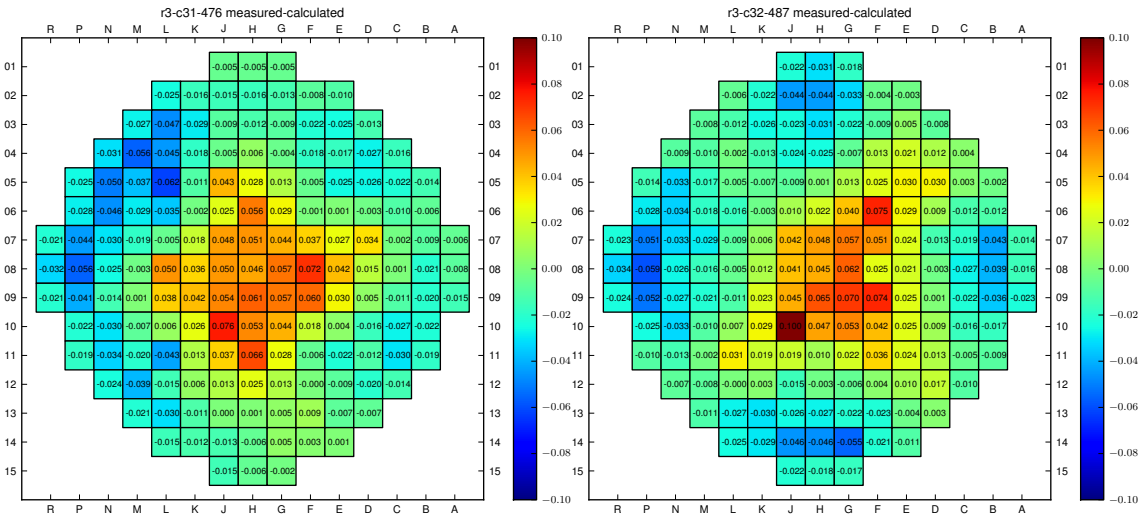


**Figure 3.7:** Absolute $F_{\Delta H}$ deviations, c31




**Figure 3.8:** Absolute $F_{\Delta H}$ deviations, c32

## 3.3 Possible Causes

Analyses performed before the work of this thesis started point towards multiple possible causes interacting [8]. The parts that will be handled in this thesis are listed below.

- Radial Power distribution
- Shielding assemblies
- Loading pattern
- Burnup-errors
- Fuel bowing
- CASMO-5 compared with CASMO-4 and SIMULATE-5 compared with SIMULATE-3.
- Radial power reconstruction

### 3.3.1 Radial Power Distribution

Each core design, corresponding to a certain cycle, result in a specific power distribution. One possibility is that some types of distributions are harder for SIMULATE to describe and that this causes the deviations. To investigate this the measured $F_{\Delta H}$ was plotted in the same radial map as previously and compared to the figures showing deviations.

To account for different power distributions in the core when looking at the deviations, a relative deviation was introduced. This means the deviations will be expressed in terms of $(measured - calculated)/measured$ values.

### 3.3.2 Shielding Assemblies

Twelve so called shielding assemblies were loaded in Ringhals 3 cycle 27 to shield the reactor pressure vessel from neutrons. These shielding assemblies have stainless steel rods in positions adjacent to the reactor vessel that reflect fast neutrons. See Figure 3.9 for the pin layout of shielding assembly. The shielding assemblies were loaded into the outermost positions, columns A and R, rows 1 and 15.

In SIMULATE-3 the assemblies are usually modelled using symmetry where only an eighth is defined in the code. This does not work on shielding assemblies since they are asymmetrical. Instead the assembly is modelled in separate quarters and assembled in SIMULATE using the FUE.SUB input card. It is possible that this modelling strategy along with steep neutron flux gradients in the shielding assemblies are causing problems in the simulator.

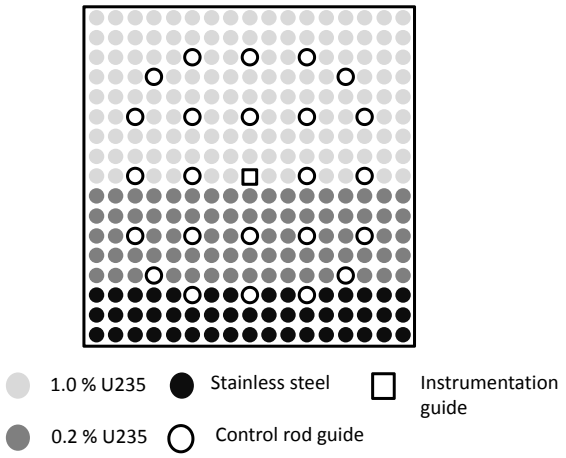


**Figure 3.9:** Pin layout of the shielding assemblies

### 3.3.3 Loading Pattern

One of the few cycle specific variables is the loading pattern where the number of new fuel assemblies and their position in the core can be varied. The core is loaded using quarter-symmetry which removes a lot of variables with regard to power distribution tilt depending on the loading pattern.

Fuel that is not fresh have been loaded in the core before which gives it a burnup history. Measuring the burnup of a fuel assembly is non-trivial, instead to get the burnup the power history of the assembly is kept track of. If the total amount of power that has been extracted from the assembly is known the burnup can be calculated. Fresh fuel does not have a history but is still dependent on correct data from the manufacturers and the neutron libraries being correct.

If the loading pattern is similar between cycles with the same deviation this may be significant. The loading pattern for the cycles leading up to cycle 32 were plotted showing the position of fresh and older fuel.

### 3.3.4 Global Burnup Error

A burnup error here is defined as when fuel that has been in the reactor for one year or longer has a different reactivity than predicted by SIMULATE. This can have many causes, either that the history of the assembly is wrong or that the assembly during that history for some reason was modelled incorrectly.

If SIMULATE calculates a too short cycle length this means that all assemblies will be more reactive in the beginning of the next cycle. The same is true of the power level. If the reactor has been running at a different power level than specified this will cause the reactivity of all assemblies to be off, since they are burned at a different rate than described. This will not be directly caught by the fluxmaps since all values are normalised against the current power level.

A measurement error from a venturi meter (measure coolant flow velocity which is used as input to the thermal power calculations) suffering from contamination

buildup has possibly been affecting Ringhals 3 since 2009. This means that the reactor power may have been between 99-100% since then, which of course will affect the burnup of all assemblies. The question is how this has affected the power distribution.

To test this the cycle length of the cycles since c27 were set to 99% of what they originally were. Since fluxmaps are taken at BOC and the only thing that noticeably affects coming cycles is burnup this is equivalent to setting the reactor power to 99%. The results show that this could indeed be part of the cause to these problems, see section 4.9.

### 3.3.5 Fluxmap Specific Burnup Error

The relative $F_{\Delta H}$ deviation was plotted against burnup. In cycle 25 and 26 the deviation has an even spread around the axis. Looking at cycle 31 and 32 however two things can be noticed; fresh fuel tend to have negative deviation while 2nd year fuel is positive. An assembly that has negative deviation one cycle also looks like it will have a positive deviation the next one. See Figures 3.10 to 3.13.

The primary reason fluxmap specific burnup error is interesting is because of the assemblies that are closest to the shielding assemblies. If they are modelled with too low power and are moved to the middle of the core this should give a higher power there, something that is not captured by SIMULATE.

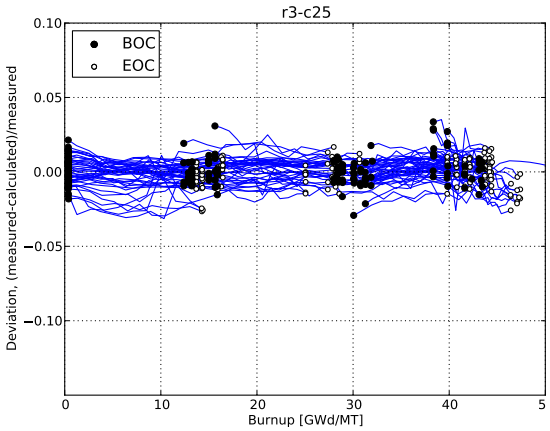


**Figure 3.10:** Relative $F_{\Delta H}$ deviations against burnup, c25

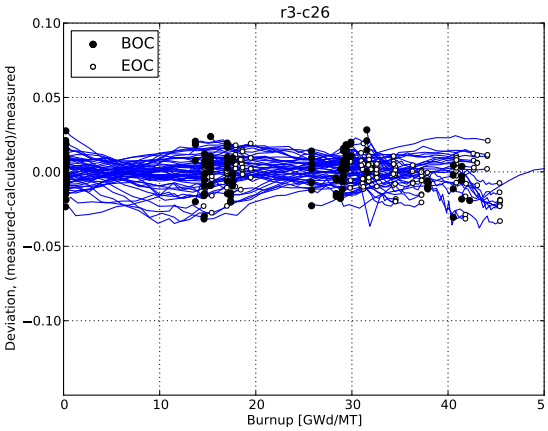


**Figure 3.11:** Relative $F_{\Delta H}$ deviations against burnup, c26

The deviation between measured and calculated $F_{\Delta H}$ causes a burnup error in SIMULATE which may affect the next cycle. It should be possible to account for this effect by tracking the history of an assembly to get an accumulated burnup error. That is, a value of the difference between the calculated burnup and a burnup that is not measured but is hopefully closer to the actual value. This in turn can be translated to a reactivity difference the assembly will have compared to the value used in SIMULATE.

See Appendix A for a flowchart description of this method. First the historical positions of every assembly is gathered. The deviation for each position is known.

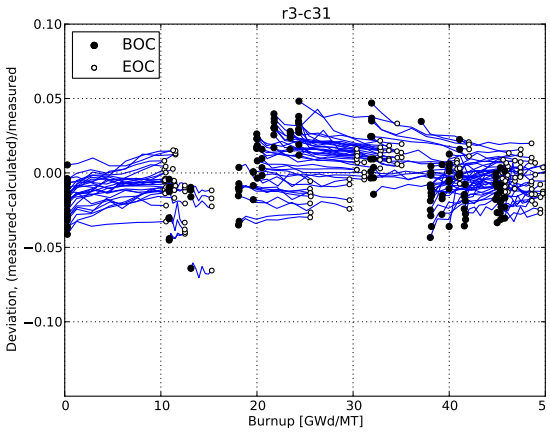


**Figure 3.12:** Relative $F_{\Delta H}$ deviations against burnup, c31

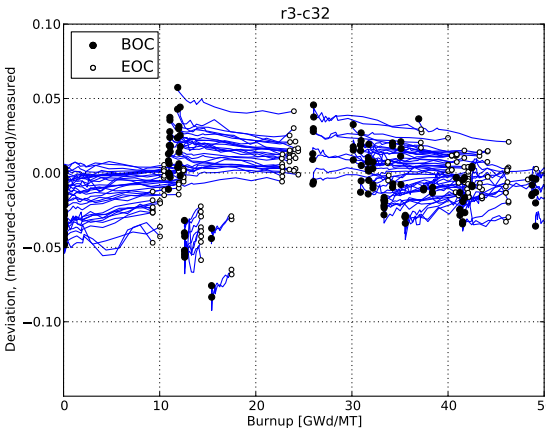


**Figure 3.13:** Relative $F_{\Delta H}$ deviations against burnup, c32

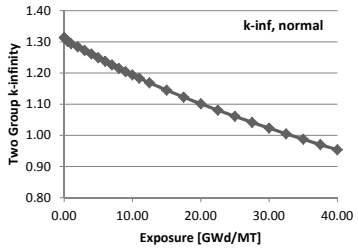


**Figure 3.14:** k-inf, standard assembly

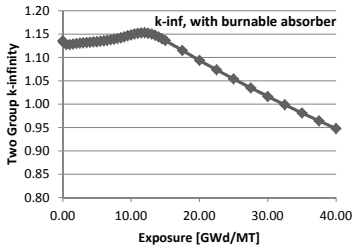


**Figure 3.15:** k-inf, burnable absorber assembly

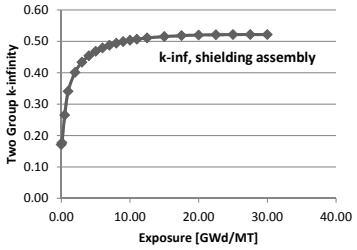


**Figure 3.16:** k-inf, shielding assembly

The normalised deviation times the specific burnup for each assembly per cycle length will give a total burnup deviation that can be summed for each assembly.

The calculated burnup for each assembly is known as well as the calculated k-inf. CASMO can produce a plot of k-inf against burnup for each assembly in the core, see Figures 3.14 to 3.16. Since one point and a difference in burnup is known a new k-inf can be interpolated from the curve corresponding to the assembly in question.

#### 3.3.5.1 FUE.XKS

SIMULATE does not accept k-inf values directly. Instead a correction is made via the card FUE.XKS which enables a modification factor for the two-group fission cross sections. The correction factor is calculated according to Equation 3.1.

$$FUE.XKS_{correction} = 1 + \frac{\text{k-inf}_{calc} - \text{k-inf}_{new}}{\text{k-inf}_{new}} \tag{3.1}$$

The FUE.XKS card should not be used in normal production according to the SIMULATE manual and the results may not be accurate [9]. But it should suffice for this type of study.

### 3.3.6 Fuel Bowing

One thing that is known to cause deviations between measured and calculated values is fuel bowing. The assemblies bow which affects the water gap between them. Since the core is moderated by water this will in turn affect the power distribution, with higher assembly power where there are bigger gaps and vice versa. Using the same method to plot $F_{\Delta H}$ for past cycles it is clear that Ringhals 3 has displayed deviation patterns in the radial power distribution before. See Figures 3.17 and 3.18 for examples of tilt that was seen in cycles 12b and 13. This type of tilt was caused by fuel bowing in the core.

There are fuel bowing measurements done after every cycle that cover some of the assemblies. The measurements done after cycle 31 indicate that there is some degree of fuel bowing, see Figure 3.19. In this plot the direction and length of the arrow corresponds to the direction of bowing and the magnitude of the bow respectively. This means cycle 32 may display deviations that are cause by fuel bowing.

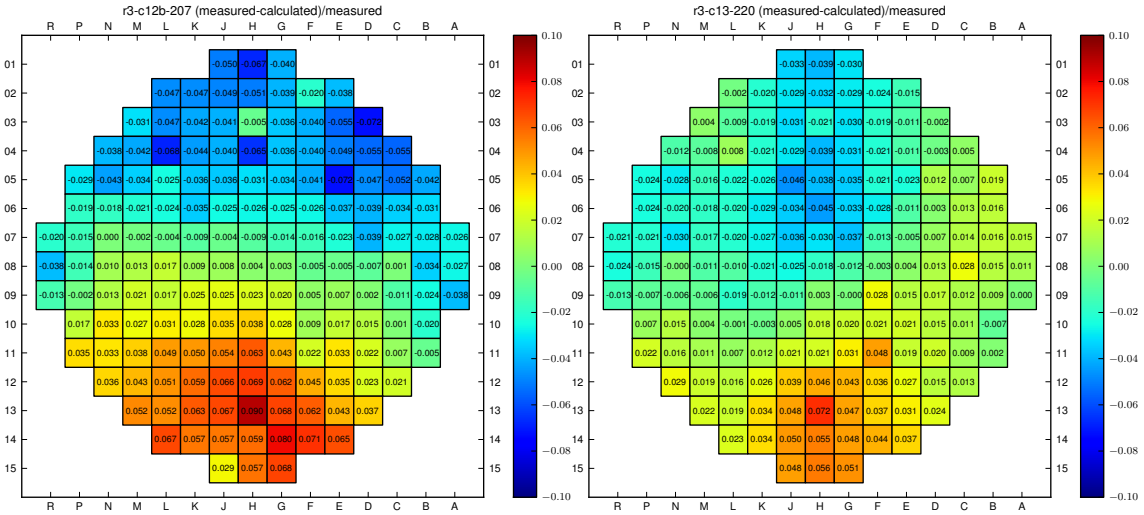


**Figure 3.17:** Absolute $F_{\Delta H}$ deviations, c12b




**Figure 3.18:** Absolute $F_{\Delta H}$ deviations, c13

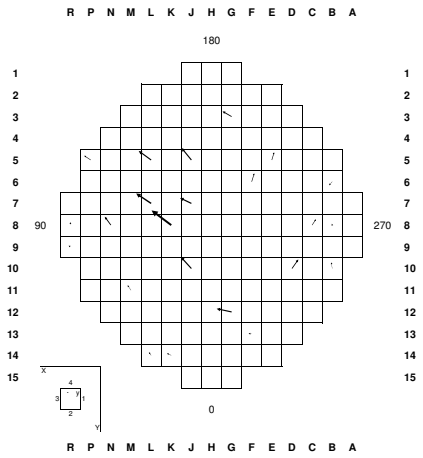


**Figure 3.19:** Fuel bowing after c31

### 3.3.7 CASMO 4/5 and SIMULATE 3/5

A major difference between the versions of CASMO used in this report is the use of different neutron libraries. CASMO-4 uses the JEF-library (Joint European File), and CASMO-5 uses the ENDF-lirary (Evaluated Nuclear Data File). It is possible that the more advanced CASMO-5 along with a better library gives a better description of the power profile.

SIMULATE-5 is a newer and more advanced version. It is possible this will give improvements in the modelling of the core.

### 3.3.8 Radial Power Reconstruction

Since the core is not measured in every position the data has to be adapted to every position. This could mean that the deviations seen are not representative of the true conditions, but rather a result from this adaptation. To test this the default values from SIMULATE were changed so that only the closest assemblies were affected by the detector.

## 3.4 Symmetric and Asymmetric Deviations

There are a lot of parameters that affect the calculations performed by SIMULATE. These include inlet temperature to the core, boron concentration, coolant flow rate and k-eff for the core. To get a better understanding of the simulations these have been varied to see if the $F_{\Delta H}$ deviations in cycle 32 could be decreased.

None of the parameters seemed to give improvements when varied within a reasonable span, but one thing became clear. Most things done in SIMULATE will affect the entire core in a symmetrical manner. This is a consequence of the core being loaded using quarter-symmetry. While this strategy is followed it seems all global parameters give an error that is symmetric.

Fuel bowing is not captured by SIMULATE which makes it hard to investigate. The fuel bowing is persistent between cycles which makes it likely that fuel bowing is a part of the error seen in cycle 32 but there is no easy way to say how large this part is. One property of the error may be possible to capture though; since the fuel bowing is asymmetrical and most other errors are symmetrical it should be possible to split the error in a symmetrical and asymmetrical part.

The symmetrical plot is made by essentially collapsing the core into one quadrant. An average power deviation is calculated for all quarter-symmetrical assemblies in the core. The individual values are then replaced by this average deviation to form a symmetrical plot. The asymmetric plot is obtained by subtracting the calculated symmetrical values from the values in the original plot. See Section 4.5 for the results of this method.

# 4
# Results

In this section the results are presented from the investigations into the possible causes laid out in the methodology.

## 4.1 Radial Power Distribution

The 2D-power distribution for each cycle was plotted, see Figures 4.1 to 4.8 (note that the scales are slightly different). Looking at the power distributions it does not seem as though higher power automatically causes deviations between measured and calculated values. There does seem to be some correlation in the overall pattern, but nothing that can explain the details. One thing that is clear however is that the magnitude of the error is affected by the assembly power level. This means that while absolute deviations are important when running the reactor, when looking at how well the core is described the relative error is what is important. The normalisation is done with the procedure: $(measured - calculated)/measured$ values.

Figures 4.9 to 4.16 show the relative version of Figures 3.1 to 3.8. The positive $F_{\Delta H}$ deviations in the centre for cycles 29, 31 and 32 are now closer in magnitude, which is a result of the later cycles having a higher power in the centre. The thing that really stands out however is the colder edges that obviously are not producing very much power. Note that the detector positions have the extreme values by definition (compare with Figure 2.2) since every other value is interpolated. This means that all the peripheral shielding assemblies (see Section 4.2 for a description) should probably be as cold as the one measured by a detector.

Another way to view this trend is by radially averaging the values and display them in a graph. See Figure 4.17 for the points used and Figure 4.18 for a condensed version of cycles 24-32. This figure displays the radially averaged deviations for every fluxmap made during the cycle, not just the first at full power. It is clear that the error picture seen from cycle 27 and onwards is unique in the reactor's history, pointing towards a change there. It also shows that the deviations tend to be biggest in the beginning of the cycle.

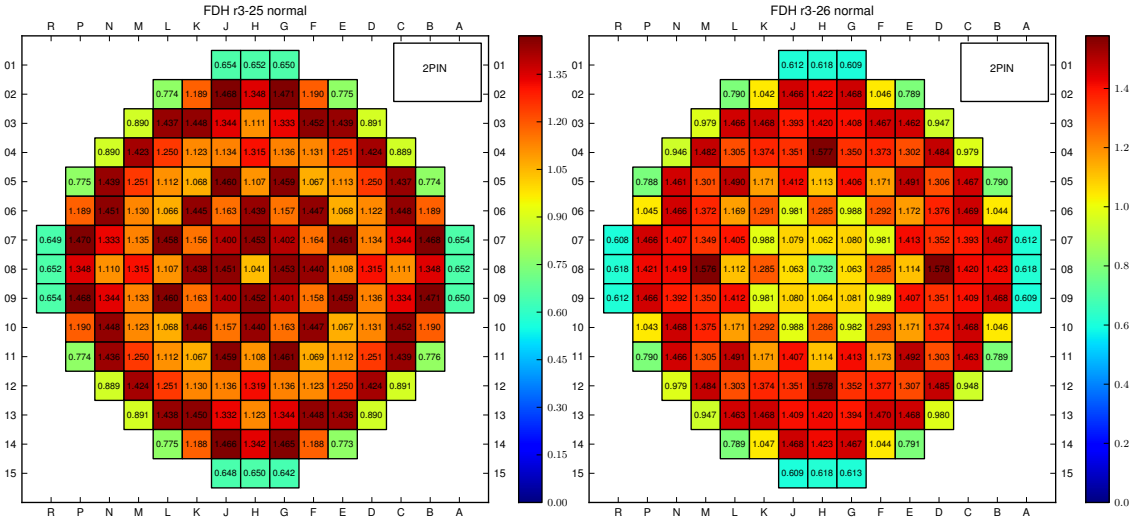


**Figure 4.1:** Measured $F_{\Delta H}$, c25




**Figure 4.2:** Measured $F_{\Delta H}$, c26

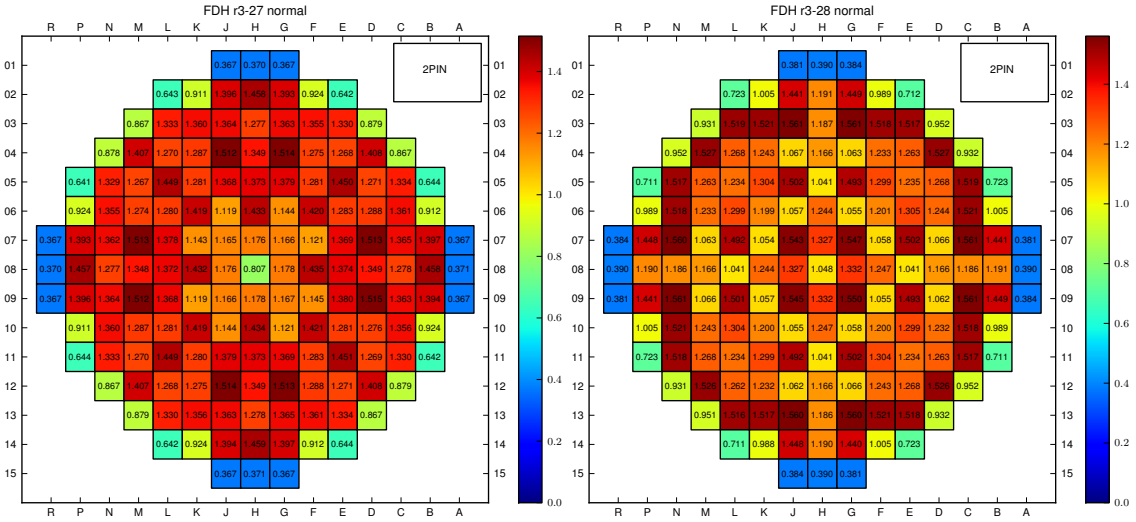


**Figure 4.3:** Measured $F_{\Delta H}$, c27




**Figure 4.4:** Measured $F_{\Delta H}$, c28

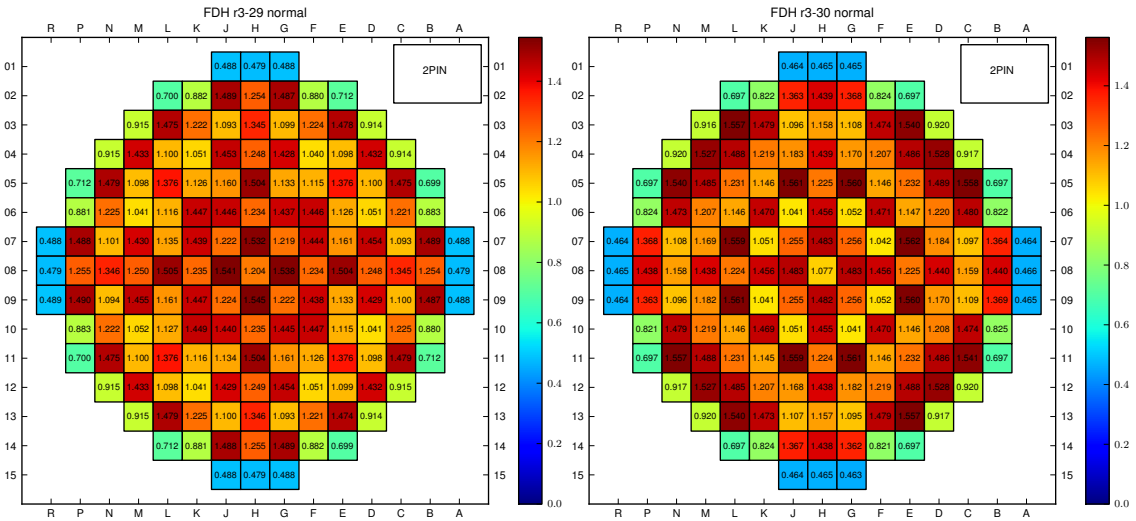


**Figure 4.5:** Measured $F_{\Delta H}$, c29




**Figure 4.6:** Measured $F_{\Delta H}$, c30

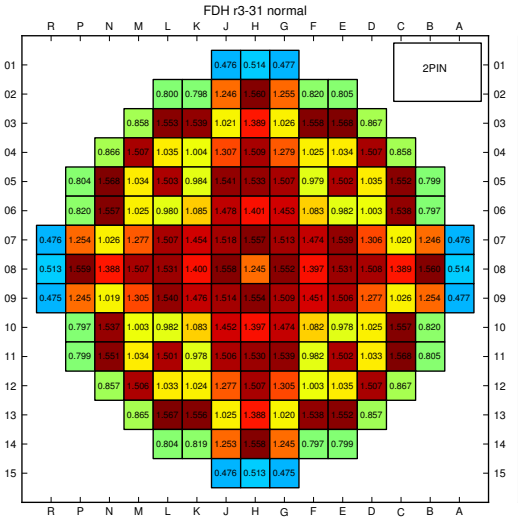


**Figure 4.7:** Measured $F_{\Delta H}$, c31

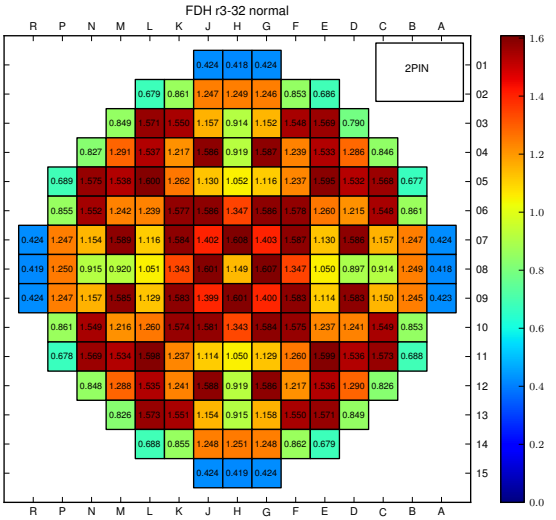


**Figure 4.8:** Measured $F_{\Delta H}$, c32

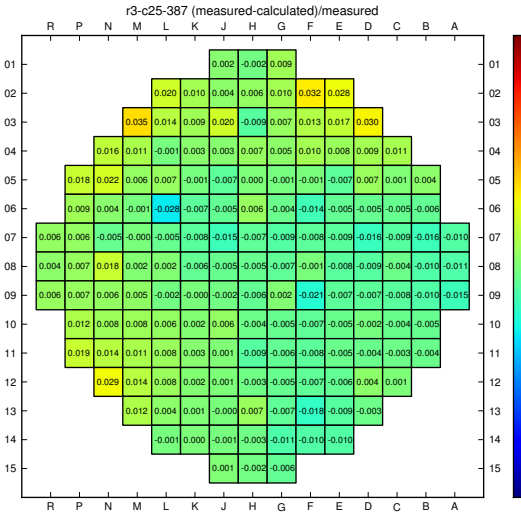


**Figure 4.9:** Relative $F_{\Delta H}$ deviations, c25

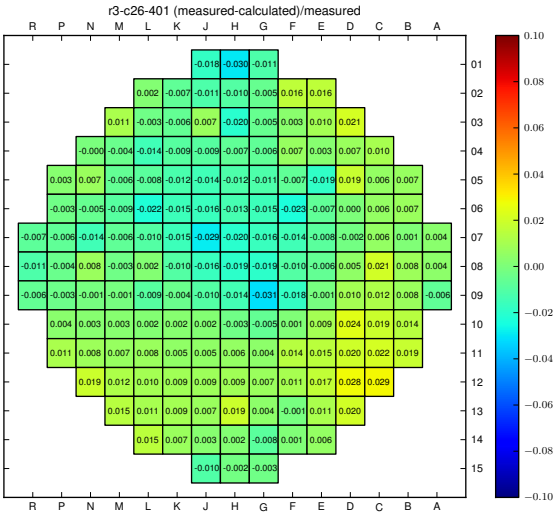


**Figure 4.10:** Relative $F_{\Delta H}$ deviations, c26

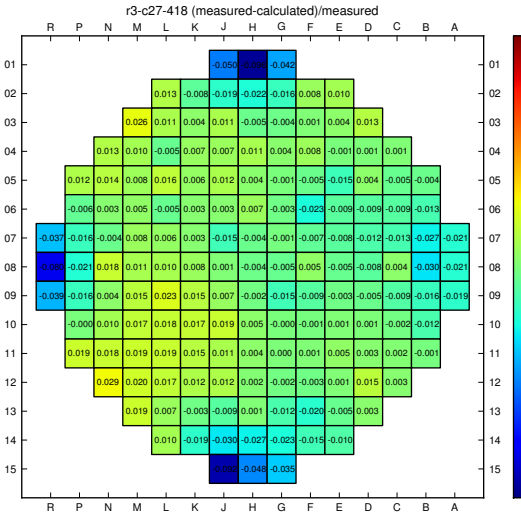


**Figure 4.11:** Relative $F_{\Delta H}$ deviations, c27

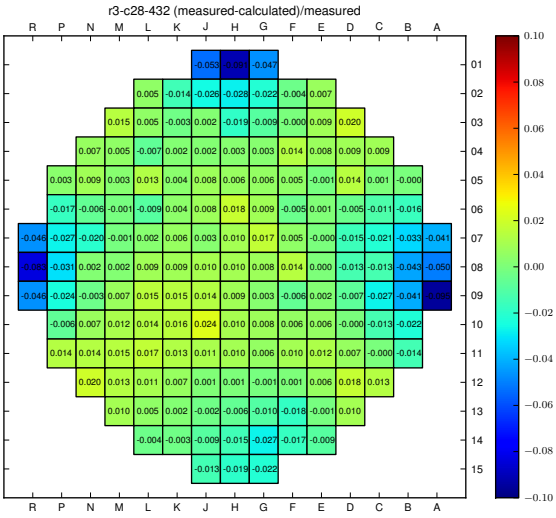


**Figure 4.12:** Relative $F_{\Delta H}$ deviations, c28

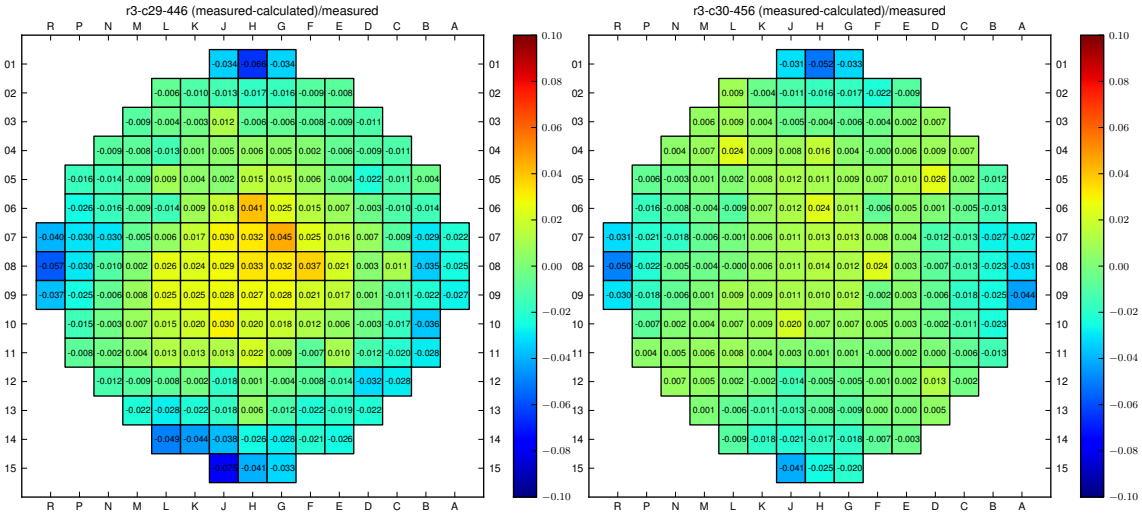


**Figure 4.13:** Relative $F_{\Delta H}$ deviations, c29




**Figure 4.14:** Relative $F_{\Delta H}$ deviations, c30

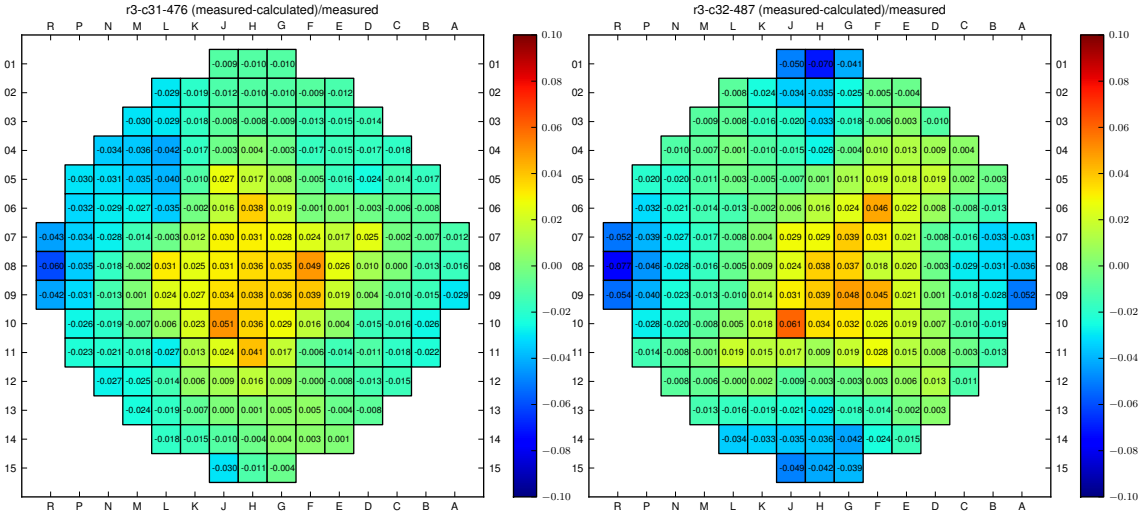


**Figure 4.15:** Relative $F_{\Delta H}$ deviations, c31




**Figure 4.16:** Relative $F_{\Delta H}$ deviations, c32

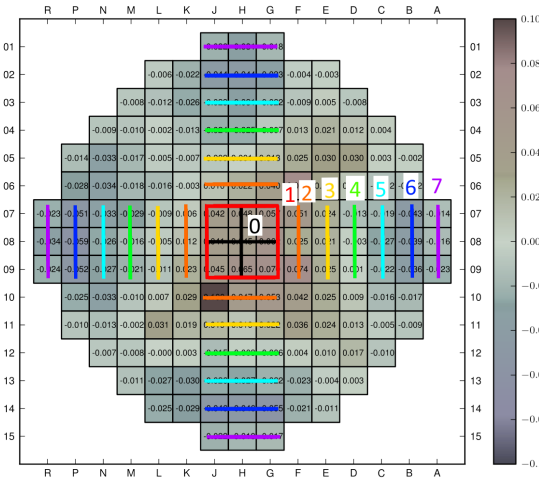


**Figure 4.17:** The values that are used to make radially averaged graph.

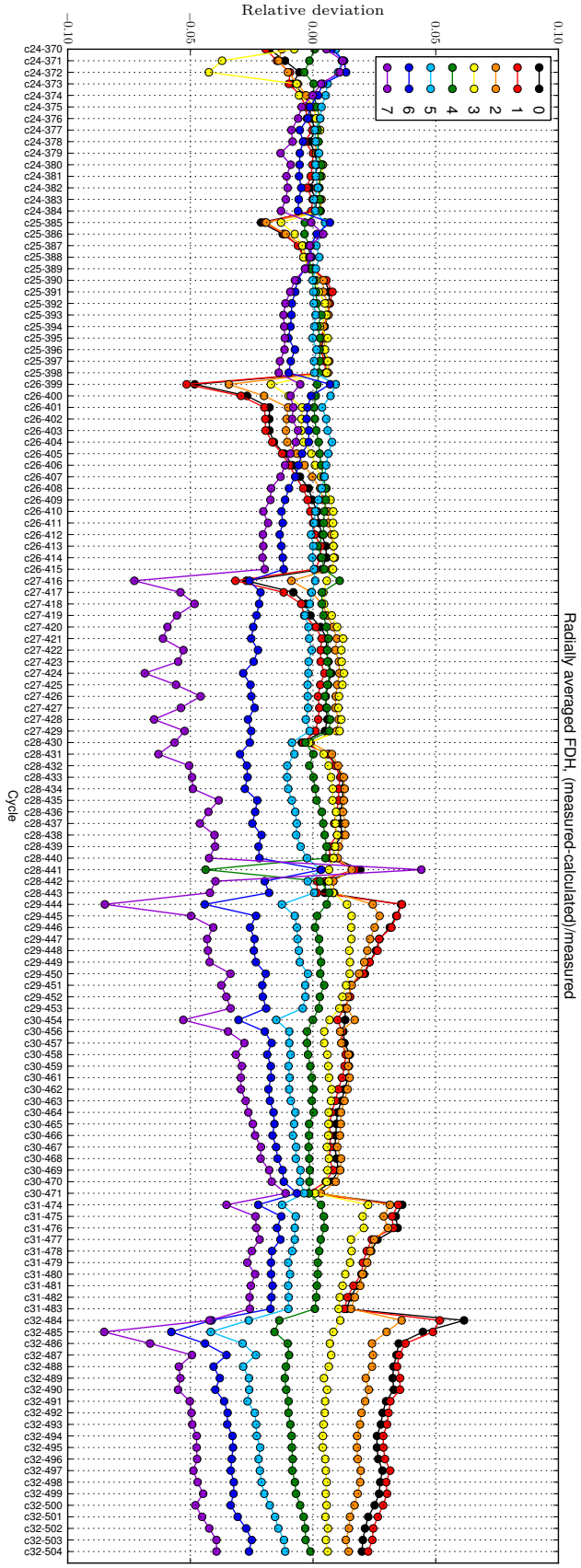


**Figure 4.18:** Radially averaged relative $F_{\Delta H}$ deviations, c24-c32

## 4.2 Shielding Assemblies

The shielding assemblies are setup correctly, but not necessarily optimally modelled, in CASMO and SIMULATE. While it is clear from the fluxmaps that they are overpredicted by the simulator no better setup has been found. Since the shielding assemblies have a very low power the effect on the rest of the core may not be that large however.

One way to test the effect of the deviations on the power distribution is to reduce the fission cross section manually with the FUE.XKS card that is present in SIMULATE. A reduction of the fission cross section by 5% in the shielding assemblies gave an increase in relative $F_{\Delta H}$ of about 0.005 evenly distributed in the core. The effect was about the same in all cycles.

## 4.3 Loading Pattern

The loading pattern for cycles 25 to 32 are shown in Figures 4.19 to 4.26. Note that fuel one cycle old is numbered 2 with the number 1 given to fresh fuel. Cycle 27 onwards the fresh and 1 year old assemblies are marked with a black triangle. These assemblies contain gadolinium rods, used as a burnable absorber (BA), that are known to give bigger uncertainties in the simulator.

A thing to note is that cycles 29, 31 and 32 have relatively few fresh assemblies loaded, and those which are loaded are loaded in the semi-peripheral positions in the core. There is nothing unusual about this loading strategy, but it does seem that fresh fuel in the centre of the core give a lower power distribution error while the configurations with fresh fuel only in the semi-periphery have a clear symmetric error. One possible explanation for this is that mixing fresh fuel and older fuel evens out an error in the description of either of them.

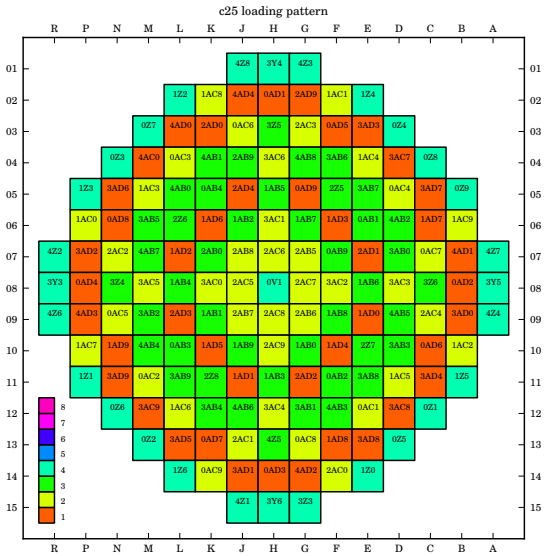


**Figure 4.19:** Loading pattern, c25

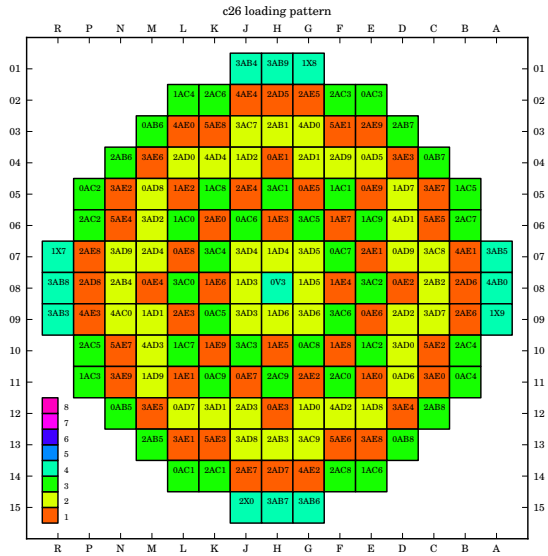


**Figure 4.20:** Loading pattern, c26

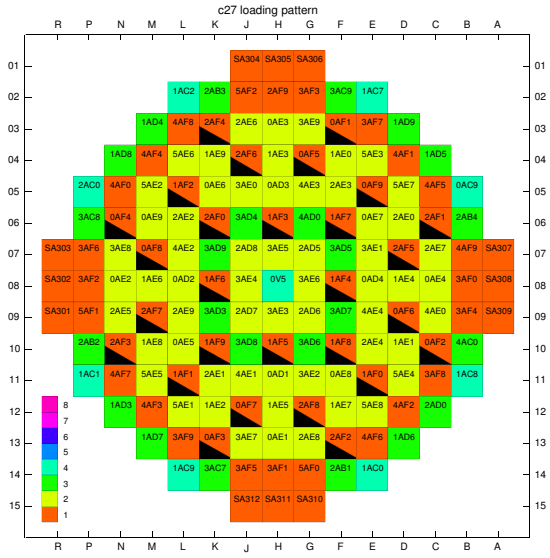


**Figure 4.21:** Loading pattern, c27. Fresh assemblies with BA marked.

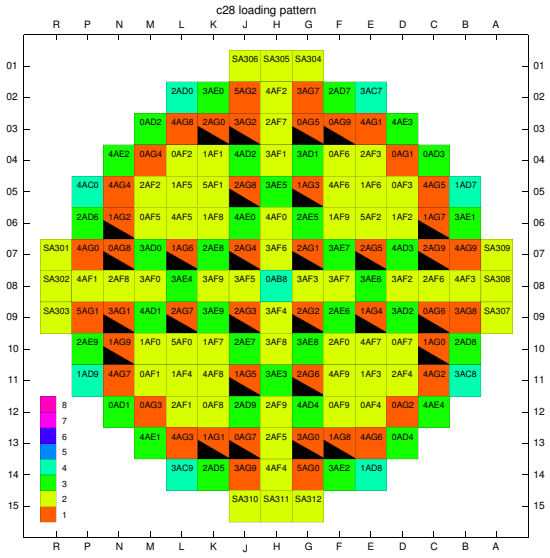


**Figure 4.22:** Loading pattern, c28. Fresh assemblies with BA marked.

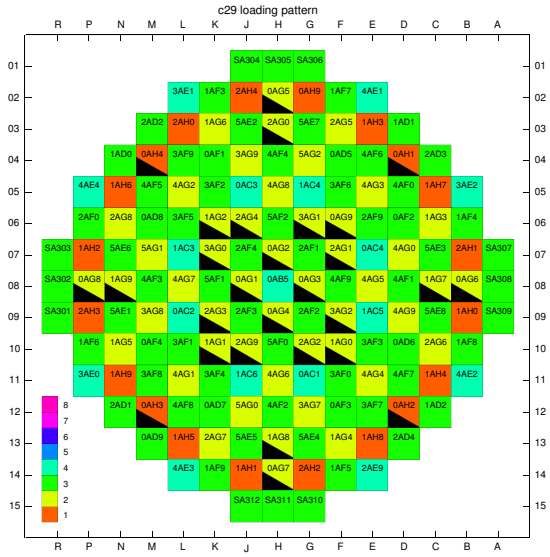


**Figure 4.23:** Loading pattern, c29. Fresh and 1 year old assemblies with BA marked.

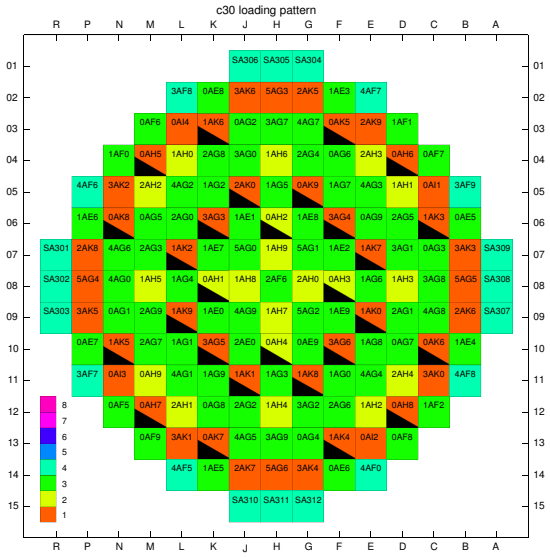


**Figure 4.24:** Loading pattern, c30. Fresh and 1 year old assemblies with BA marked.

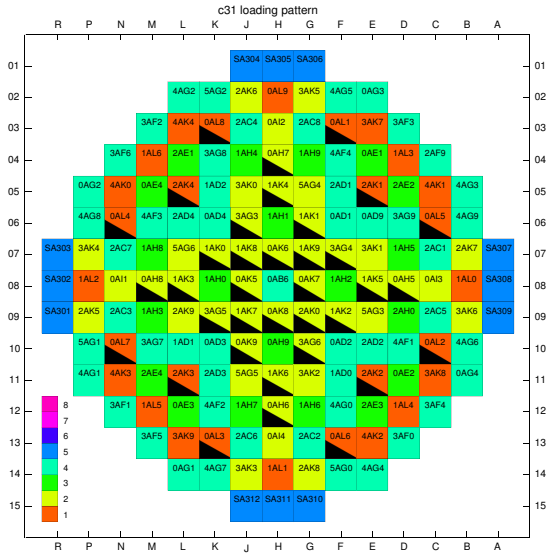


**Figure 4.25:** Loading pattern, c31. Fresh and 1 year old assemblies with BA marked.

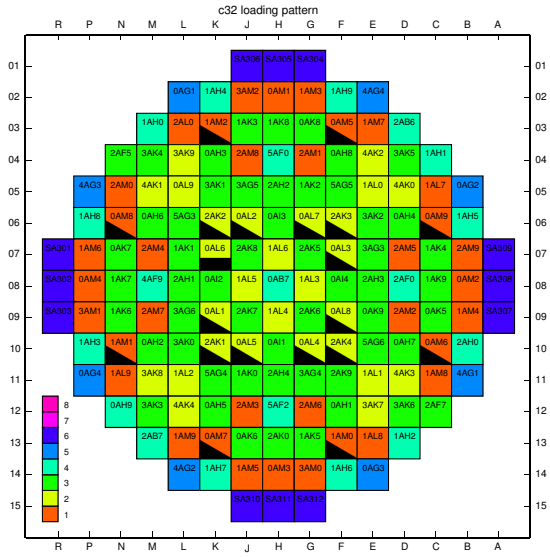


**Figure 4.26:** Loading pattern, c32. Fresh and 1 year old assemblies with BA marked.

## 4.4 Results from Burnup Correction

The FUE.XKS maps were input to SIMULATE starting at cycle 28 since this was the first cycle where assemblies had been close to the shielding assemblies. Here only the correction maps from cycle 29 to 32 are shown however, see Figures 4.27 to 4.30.

The results from the accumulated burnup-correction show that the general pattern in cycles 29, 31 and 32 can not be explained by a burnup error caused by deviations displayed in the fluxmaps. For cycle 32 the burnup error may have added to the underlying pattern causing larger deviations. Further investigation into this revealed that for cycle 32 there were assemblies moved into the middle that had been located next to the shielding assemblies for two cycles.

The magnitude of this error is very uncertain however, since the method is not very precise. It may reduce the deviation in relative $F_{\Delta H}$ for cycle 32 with up to 0.01 in the critical position J-10.

## 4.5 Fuel Bowing

Figures 4.31 and 4.32 show the result when Figure 4.16 is split up into a symmetric and asymmetric part. Almost half of the error in position J-10 is in the asymmetric graph. The important conclusion from this result is that a big part of the error will not be possible to explain with a burnup error or some global variable in SIMULATE.

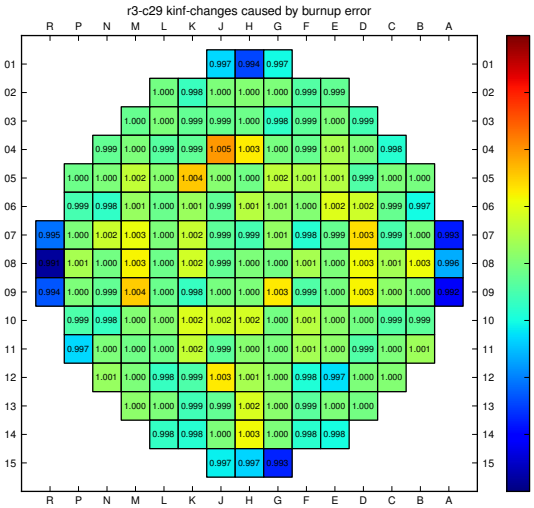


**Figure 4.27:** kinf-change, c29

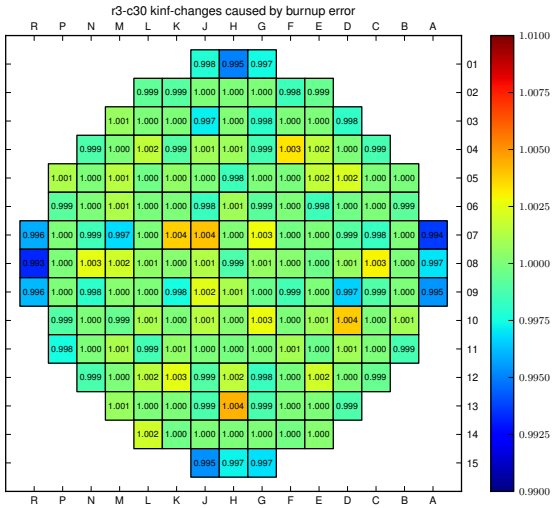


**Figure 4.28:** kinf-change, c30

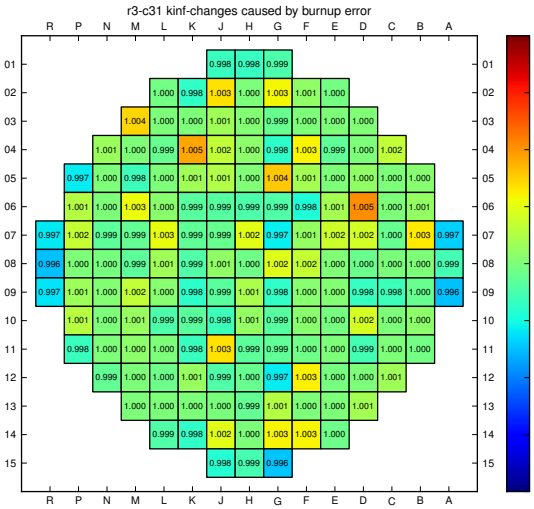


**Figure 4.29:** kinf-change, c31

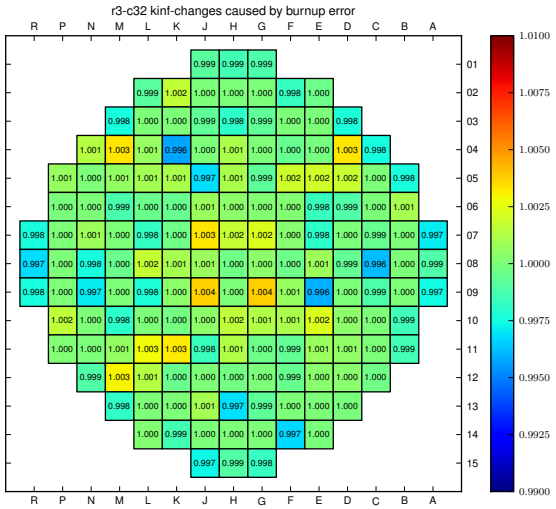


**Figure 4.30:** kinf-change, c32

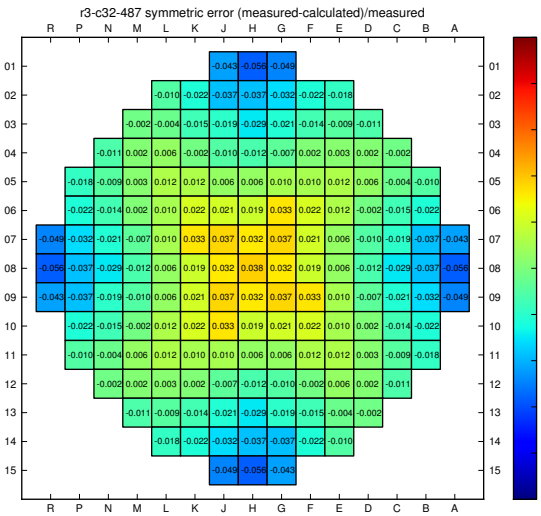


**Figure 4.31:** Symmetric relative $F_{\Delta H}$ deviations, cycle 32

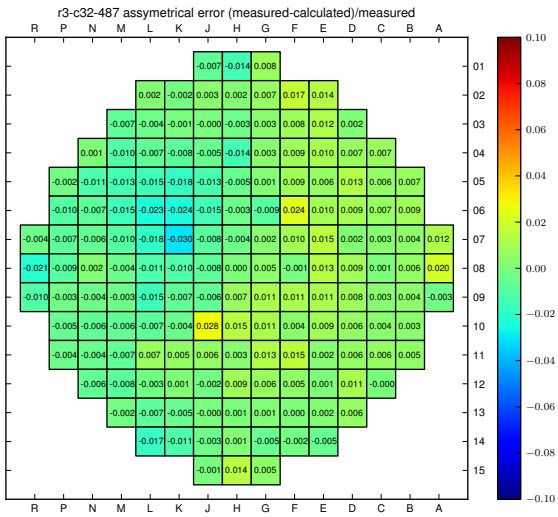


**Figure 4.32:** Asymmetric relative $F_{\Delta H}$ deviations, c32

## 4.6 CASMO-5

All previous cycles were rerun with CASMO-5 and a new library ENDF B VII. SIMULATE-3 was still used to run the cycles which means the only difference is the neutron cross sections. See the effect of those changes in Section 4.9.

## 4.7 SIMULATE-5

In addition to CASMO-5 a few tries were done with SIMULATE-5 as well. This software is still not fully integrated to the surrounding systems which means the results had to be displayed in terms of absolute difference in RPF, relative power fraction.

The biggest difference between RPF and FDH (both absolute difference) is seen in the shielding assemblies. This is because they experience a large power gradient with big difference between hottest and coldest channel. They have a small relative power compared to the hottest channel enthalpy.

Figure 4.33 is the RPF version of Figure 3.3. Figure 4.34 and Figure 4.35 are the same results from a CASMO-5/SIMULATE-3 run extracted in a different way where the latter does not have ADAPT to extrapolate the data.

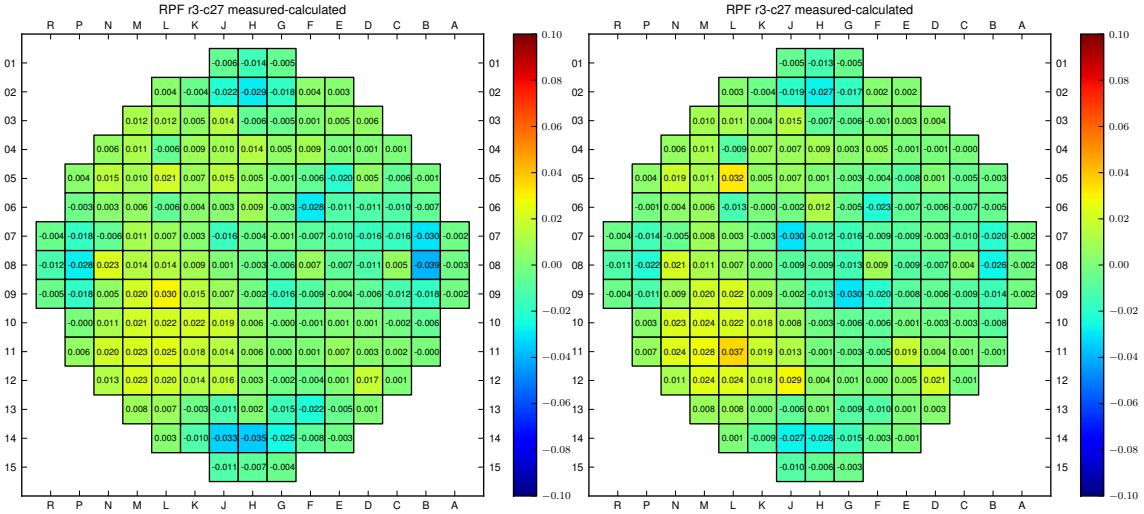


**Figure 4.33:** Absolute RPF deviations, C4S3, c27




**Figure 4.34:** Absolute RPF deviations, C5S3, c27

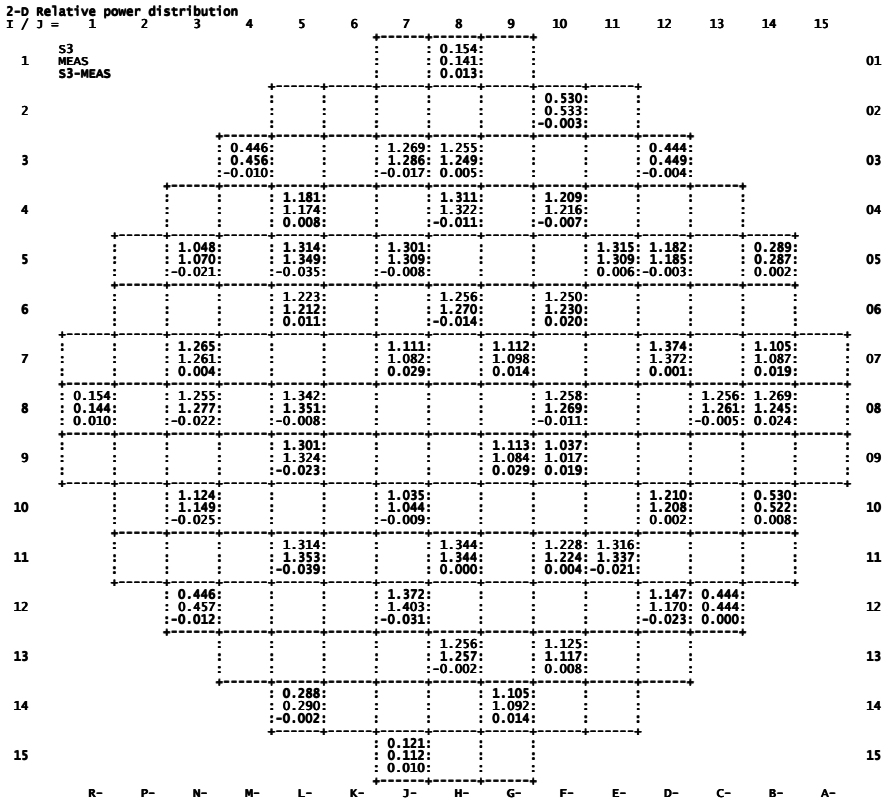


**Figure 4.35:** Absolute RPF deviations, C5S3, c27

These figures show three values in each position: *simulated*, *measured* and *simulated* − *measured* (which is the opposite of the colour plots). SIMULATE-5 does seem to give better agreement with measurements in the shielding assemblies for cycle 27, compare Figure 4.36 to Figure 4.35.

The are some improvements for the shielding assemblies in cycle 31, compare Figures 4.37 to 4.38. The centre has a higher deviation when using SIMULATE-5 however, indicating that the modelling of shielding assemblies and high deviations in the centre are separate issues.

## 4.8 Radial Power Reconstruction

The change of weighting factors had an effect on the power distribution. The difference can be seen by comparing Figure 4.39 to the old one which is Figure 4.40. As can be seen the result is a shape that has bigger changes locally. What is correct has not been investigated, but it is clear that the non-detector positions are dependent on this algorithm. Close to the shielding assemblies the modified values can be argued to be more correct since the difference in power is biggest there. The overall deviation shape is not affected though, which means this the power adaptation can be written off as a source of the error.

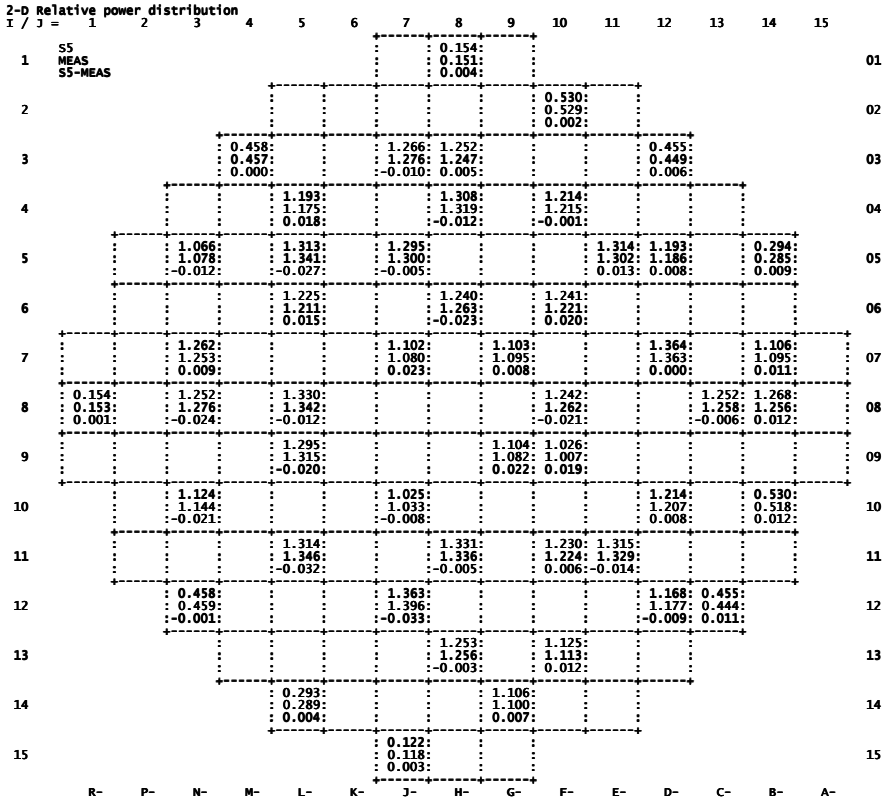


**Figure 4.36:** Absolute RPF deviations, C5S5, c27

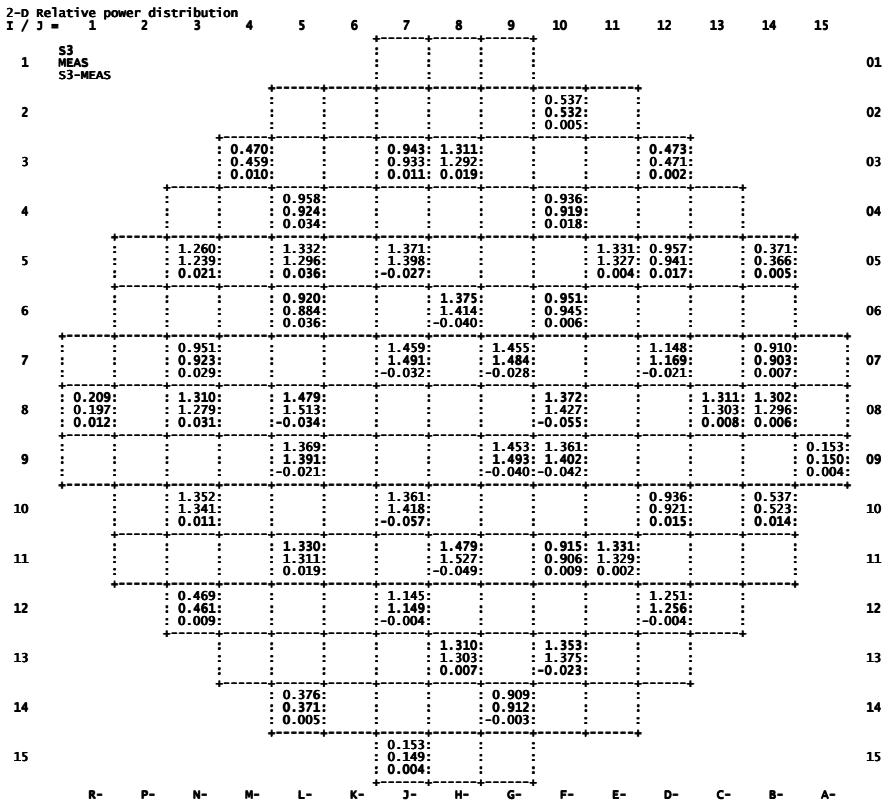


**Figure 4.37:** Absolute RPF deviations, C5S3, c31

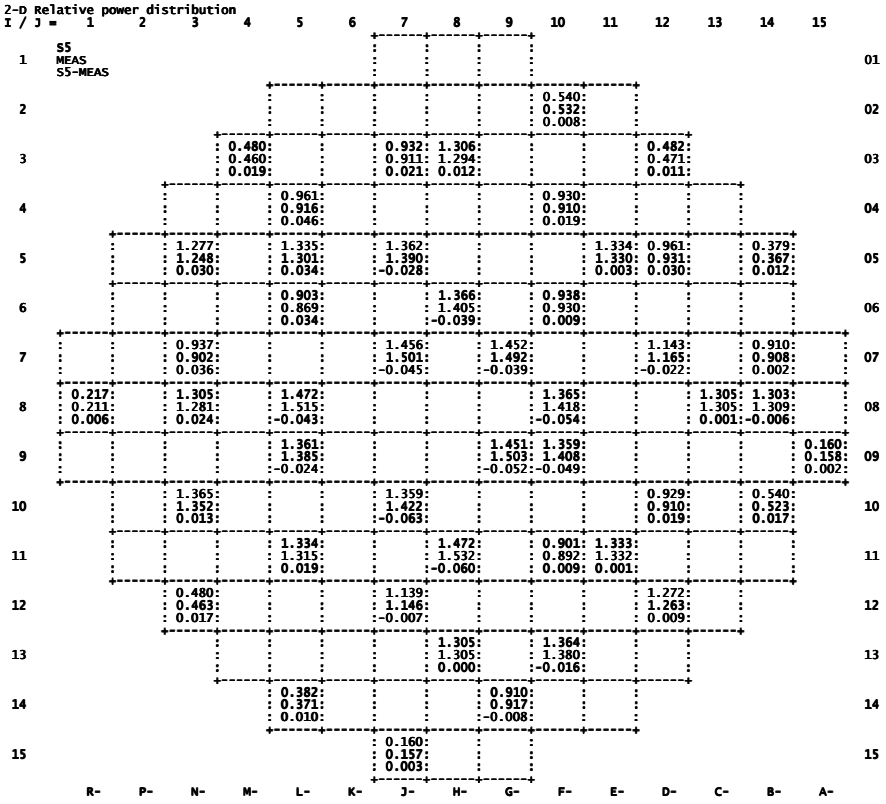


**Figure 4.38:** C5S5 relative power fraction, c31.

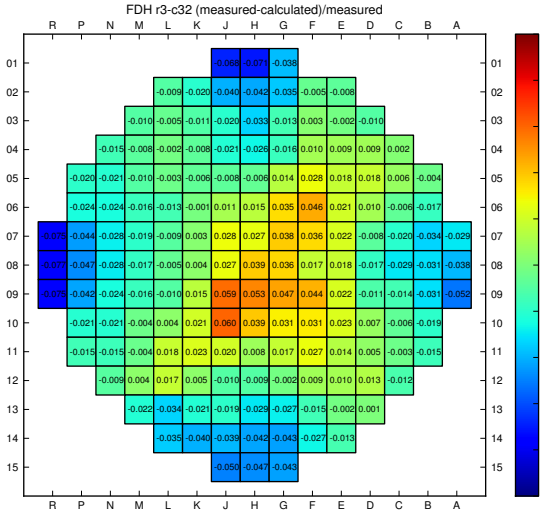


**Figure 4.39:** Relative $F_{\Delta H}$ deviations with the modified weighting factors.

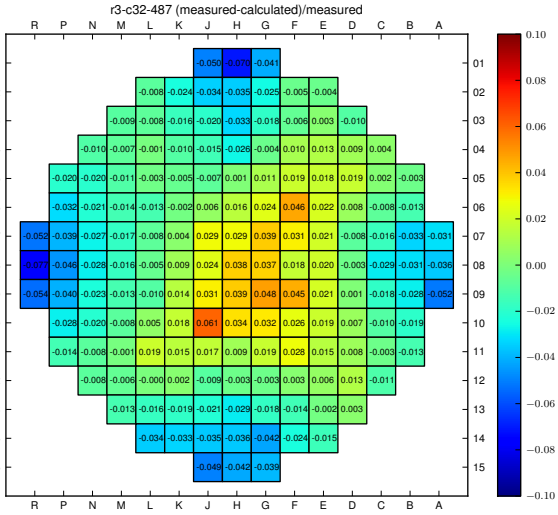


**Figure 4.40:** Relative $F_{\Delta H}$ deviations with default weighting factors.

## 4.9 Effects on Symmetric Error

Changes to the simulations does not seem to affect the asymmetric errors in a significant way. This behaviour is expected if the cause of the deviations is fuel bowing because it is not included in the simulations. Efforts to reduce asymmetric errors will have to be made in the physical reactor, and predicted and taken into account in the simulations. The symmetric errors however have shown to be affected by changes to the simulations. See Figures 4.41 to 4.46 for the symmetric errors of the last few few cycles using the original modelling with CASMO-4 and SIMULATE-3. The asymmetric errors are shown in Appendix B.

The results displayed in this section will thus show things that affect the symmetric error shown in cycles 29, 31 and 32. The positions and relative magnitude of the deviations are very similar which means there is most likely a common cause to the problem.

When CASMO 5 with the ENDF library was used, the shape and magnitude of the deviations were affected. The fresh assemblies seemed to be less reactive in CASMO-5 when compared to CASMO-4. The biggest changes was seen in cycles 29, 31 and 32 indicating that this type of loading pattern is more sensitive to disturbances. The same thing has been seen when power was set to 99%, these cycles are affected the most. Table 4.1 show the maximum value from the symmetric plots with these changes.

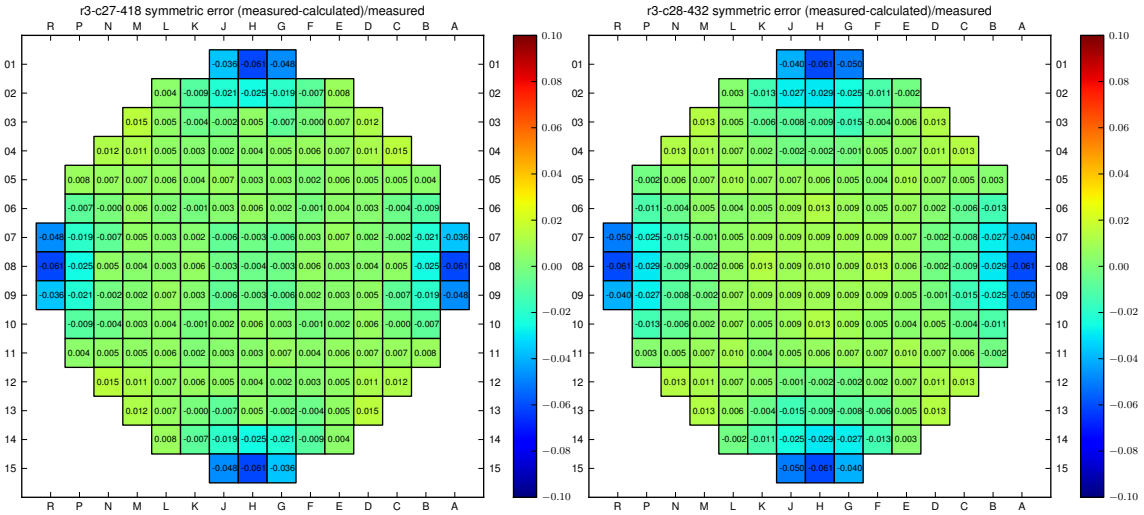


**Figure 4.41:** Symmetric relative $F_{\Delta H}$ deviations, c27




**Figure 4.42:** Symmetric relative $F_{\Delta H}$ deviations, c28

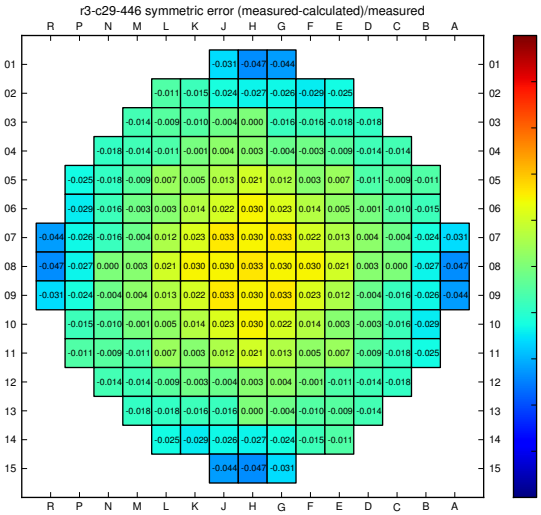


**Figure 4.43:** Symmetric relative $F_{\Delta H}$ deviations, c29

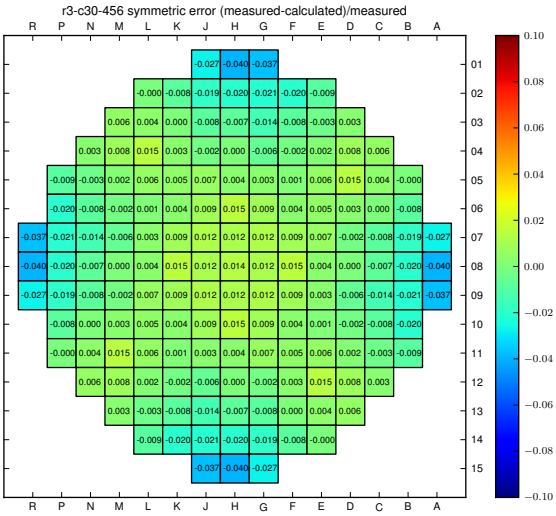


**Figure 4.44:** Symmetric relative $F_{\Delta H}$ deviations, c30

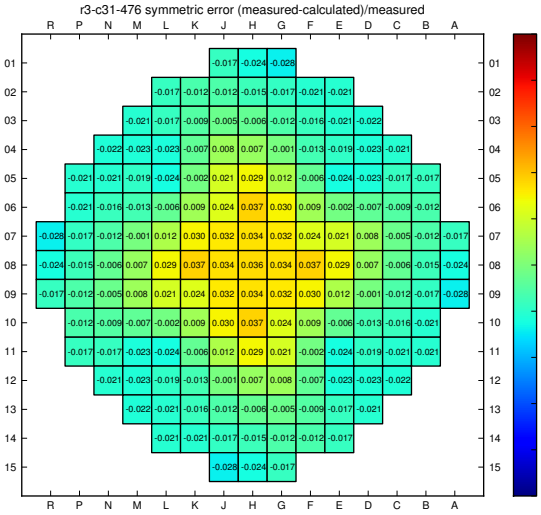


**Figure 4.45:** Symmetric relative $F_{\Delta H}$ deviations, c31

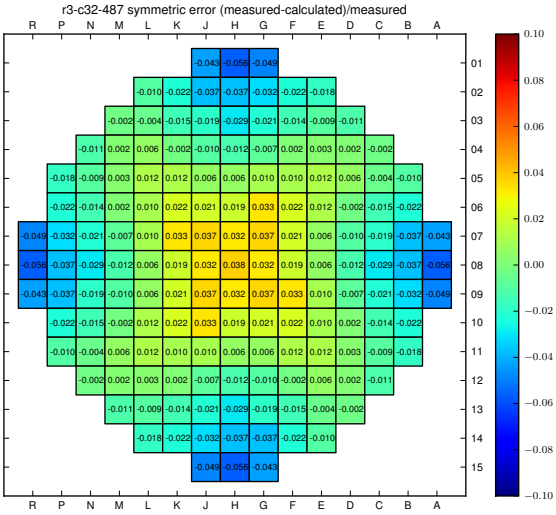


**Figure 4.46:** Symmetric relative $F_{\Delta H}$ deviations, c32

**Table 4.1:** The highest symmetric value for relative $F_{\Delta H}$ deviations.

| Cycle | Max deviation (C4/S3) | C5/S3 | C5/S3 + 99% power |
|---|---|---|---|
| c27 (M-3) | 0.015 | 0.015 | 0.015 |
| c28 (M-3) | 0.013 | 0.014 | 0.015 |
| c29 (H-8) | 0.033 | 0.027 | 0.023 |
| c30 (L-4) | 0.015 | 0.018 | 0.019 |
| c31 (K-8) | 0.037 | 0.029 | 0.022 |
| c32 (H-8) | 0.038 | 0.028 | 0.023 |

# 5
# Discussion and Conclusions

## 5.1 Discussion

The symmetric error has been shown to be affected by various factors in SIMULATE. Running with the cross sections generated by CASMO-5 significantly reduced the deviations for cycles 29, 31 and 32. This is presumably because of the change of neutron library. The new library seemed to affect fresh assemblies the most, they were less reactive. The effect on older assemblies is not as clear.

Lower thermal power along with CASMO-5 reduced the error to the point where cycle 32 no longer looked very special. The remaining error may be close to the accuracy of the simulator where only the shape of the error distribution is changing between cycles. The difference in loading pattern seems to be the one of the main contributors to this phenomenon. Some configurations are also significantly more sensitive to disturbances than others.

There are weaknesses with the symmetric and asymmetric approach. A measurement error in one assembly may cause the average deviation of the four quarter-symmetric assemblies to deviate a lot from what it should be. Thus every assembly will get an asymmetric error when it really should only be applied to the one with the measurement error. It is important to remember this when analysing the plots.

Measurement errors have not been handled in this thesis. Position J-10 is the position with the highest deviation in cycle 31 and 32, which could possibly be due to a measurement error. The detectors are calibrated during the measurements however which makes recurring erroneous measurements unlikely. This possible cause of the deviation in position J-10 was thus discarded.

SIMULATE-5 gave no improvements but showed along with the FUE.XKS tests that the shielding assemblies may not be a big issue when looking at the full picture. Since they have a negative deviation in the SIMULATE-3 runs they probably cause a slightly more positive deviation in the middle, but no more dramatic than seen in cycles 27 and 28.

The burnup correction experiment that tried to correct for each individual assembly gave uncertain results, but they were interesting nonetheless. Cycle 32 was the only one that was affected which gives an additional source of deviations for that cycle. A side effect is that if this was not the case cycle 31 would probably have had the biggest deviations.

## 5.2 Conclusions

The deviations between measured and calculated peaking factors can be split into symmetric and asymmetric components. Asymmetric deviations will not be affected by changes in SIMULATE because of how global parameters affect the quarter-symmetrical loading pattern. The asymmetric error seen in cycle 32 gave a high deviation in a high power position. This deviation would have almost caused the exceeded $F_{\Delta H}$ limit by itself.

The loading pattern has a large effect on the symmetric error. The underlying cause is that fresh and older fuel assemblies are not modelled with the same accuracy. It has been shown that a correction of older assemblies have an effect, as does changing the neutron library. A possible burnup error in assemblies adjacent to the shielding assemblies was found less important.

The best results were calculated by CASMO-5 and SIMULATE-3 with corrected thermal power. Setting up the model in SIMULATE-5 did not reduce the deviation in the critical position.

### 5.2.1 Recommendations

The recommendations can be split up into two parts: how to get the best conditions for core physics calculations and how to continue the work to figure out the cause of the deviations in $F_{\Delta H}$.

To avoid big deviations it is recommended to load fresh fuel evenly distributed in the core. It is also recommended to use CASMO-5 with the ENDF B VII neutron library and to make sure the simulator is running at the correct thermal power.

To continue working on the root cause it is recommended to keep using the symmetric and asymmetric plots to keep different causes of the deviations separated. The symmetric errors can be used to follow up the effect of the loading pattern on the power distribution. Further study is recommended on fuel bowing and on other things that may cause an asymmetric tilt in the core. The fuel bowing measurements could be used to try to predict the asymmetric deviations in the coming cycle.

# Bibliography


[1] *Technical information on Ringhals*, Vattenfall, Ringhals AB. [Online]. Available: `corporate.vattenfall.se/globalassets/sverige/om-vattenfall/om-oss/var-verksamhet/ringhals/pdf/teknisk-engelsk-2014.pdf` (visited on 08/05/2015).

[2] C. Demaziére, *Physics of Nuclear Reactors*, Lecture notes, TIF210, Division of Nuclear Engineering, Department of Applied Physics, Chalmers University of Technology, Gothenburg, Sweden 2013.

[3] ——, *Reactor Calculation Methodology*, Lecture notes, TIF195 - Applied Nuclear Engineering, Division of Nuclear Engineering, Department of Applied Physics, Chalmers University of Technology, Gothenburg, Sweden 2014.

[4] D. Knott, B. H. Forssén & M. Edenius, *Casmo-4 methodology*, SOA-95/2, Studsvik Scandpower, 1995.

[5] J. T. Cronin, K. S. Smith & D. M. Ver Planck, *Simulate-3 methodology*, SOA-95/18, Studsvik Scandpower, 1995.

[6] *Härddrift*, R34-ROK-001, Ringhals AB, Kärnkraftsäkerhet och Utbildning AB, 2001.

[7] T. Bahadir, *PWR detector comparison model*, SSP-01/459, Studsvik Scandpower, 2001.

[8] U. Svensson, *R3 Orsaksanalys - Gränsvärde för radiell formfaktor överskriden vid uppstart av cykel 32*, ID=2286947, Ringals (internal), 2014-07-02.

[9] L. J. Covington, D. M. Ver Planck & J. A. Umbarger, *Simulate-3 user's manual*, SOA-95/15, Studsvik Scandpower, 1995.

# A

# Fluxmap specific burnup

## For all assemblies in the core:

**Known:**
Total burnup

**Track history and calculate deltaB:**
Normal deviation per cycle (from fluxmap in middle of cycle)
Specific burnup/cycle
deltaB = Normal deviation•specific burnup

**Sum history**
deltaB_tot = $\sum$ deltaB

**Read (interpolate) k_inf from graph**
Total Burnup gives kinf
Total Burnup + deltaB
gives kinf_new

**Calc correction factor**
1 + (kinf_new – kinf)/kinf_new

## Example:

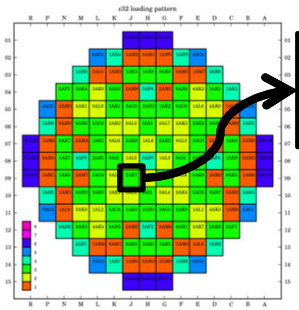

**Assembly 2AK7**
C32 position: J9
Total burnup: 26 GWd/tHM

C31 position: B7
Normal deviation: –0.011
Specific burnup: 7.4 GWd/tHM
deltaB = –0.0814 GWd/tHM

C30 position: J14
Normal deviation: –0.024
Specific burnup: 17.5 GWd/tHM
deltaB = –0.42 GWd/tHM

7.4 + 17.5 < 26, see *

deltaB_tot = deltaB_31 + deltaB_30 =
–0.5014 GWd/tHM

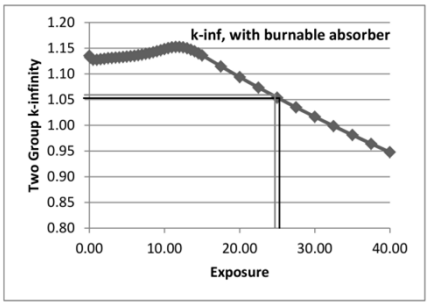


kinf = 1.054
Kinf_new=1.058
1 + (kinf_new – kinf)/kinf_new = 1.0038

* The burnup data comes from fluxmaps. The last fluxmap is taken a couple of weeks before EOC which means a small part of the total burnup will be unaccounted for.

# B
# Asymmetric errors

Asymmetric errors for cycles 27 to 32.

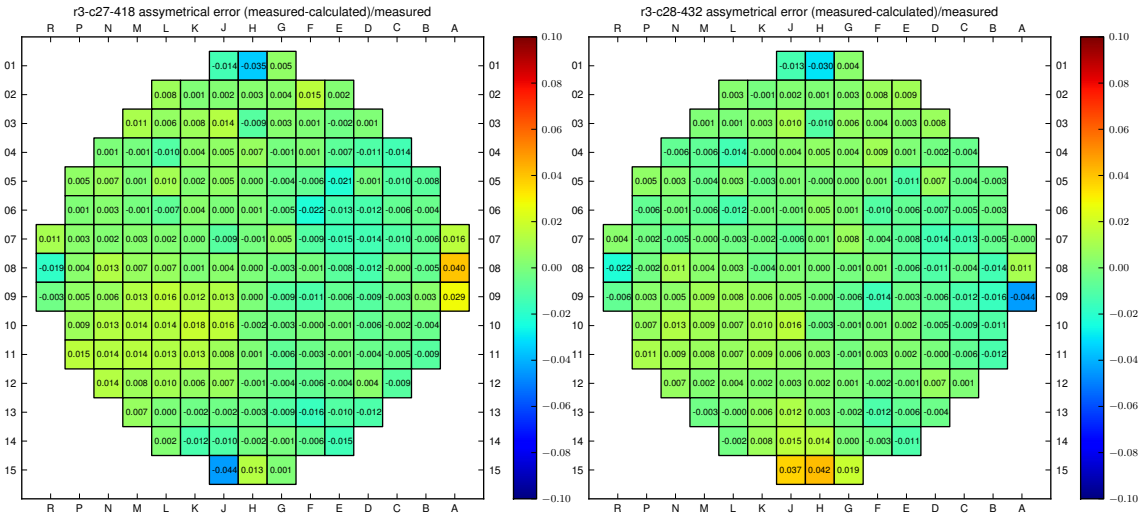


**Figure B.1:** Asymmetric relative $F_{\Delta H}$ deviations, c27




**Figure B.2:** Asymmetric relative $F_{\Delta H}$ deviations, c28

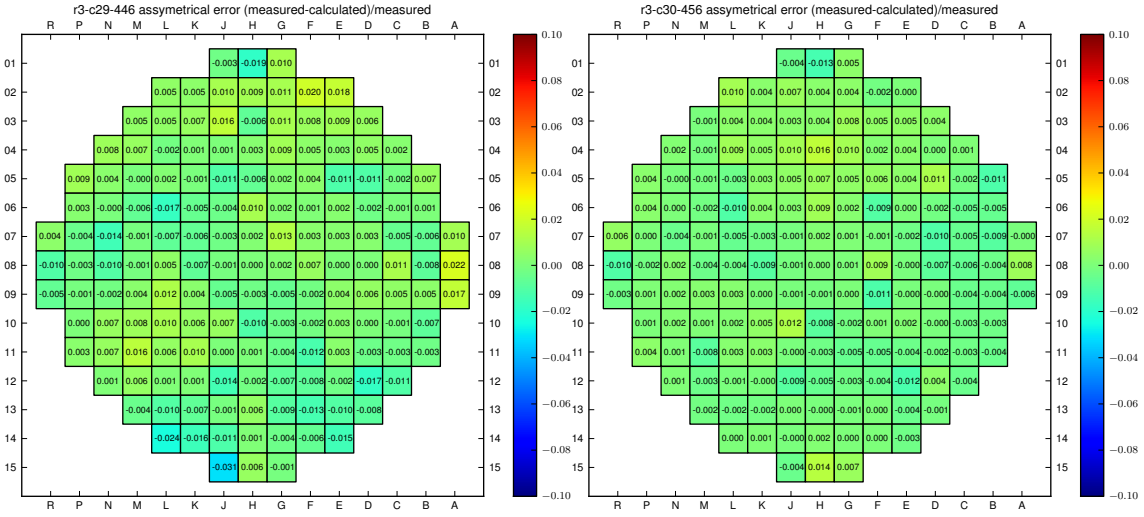


**Figure B.3:** Asymmetric relative $F_{\Delta H}$ deviations, c29




**Figure B.4:** Asymmetric relative $F_{\Delta H}$ deviations, c30

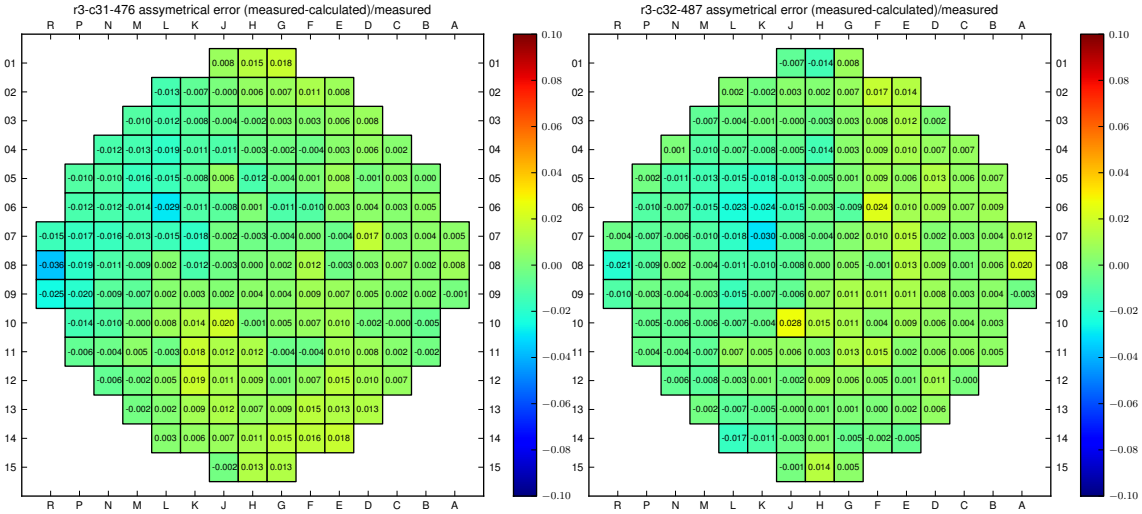


**Figure B.5:** Asymmetric relative $F_{\Delta H}$ deviations, c31




**Figure B.6:** Asymmetric relative $F_{\Delta H}$ deviations, c32